

***Physics 224 - Spring 2010***

**Week 5**  
**DARK MATTER;**  
**TOPOLOGICAL DEFECTS**

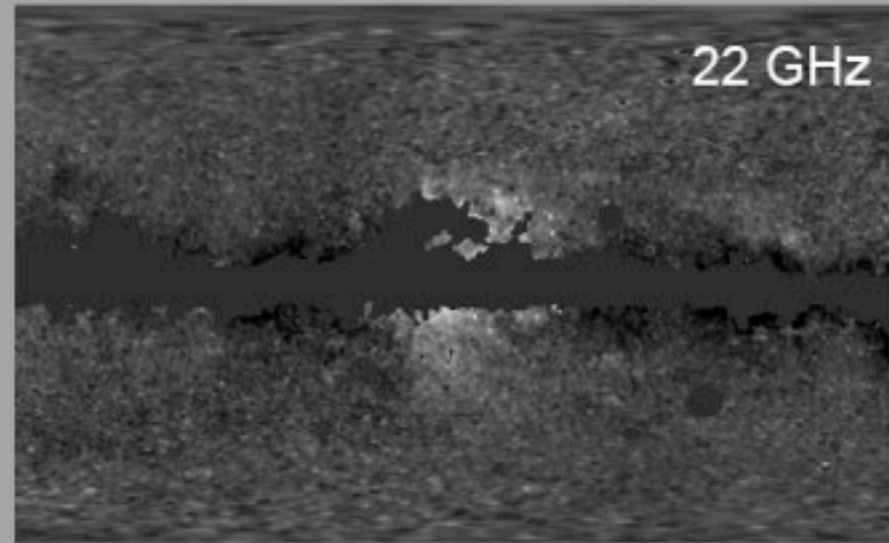
**Joel Primack**

**University of California, Santa Cruz**

[WARNING: don't take the next few slides too seriously!]

# Dark Matter in the WMAP Sky

• In 2004, Doug Finkbeiner suggested that the WMAP Haze could be synchrotron from electrons/positrons produced in dark matter annihilations in the inner galaxy (astro-ph/0409027)



• In particular, he noted that:

1) Assuming an NFW profile, a WIMP mass of 100 GeV and an annihilation cross section of  $3 \times 10^{-26} \text{ cm}^3/\text{s}$ , the total power in dark matter annihilations in the inner 3 kpc of the Milky Way is

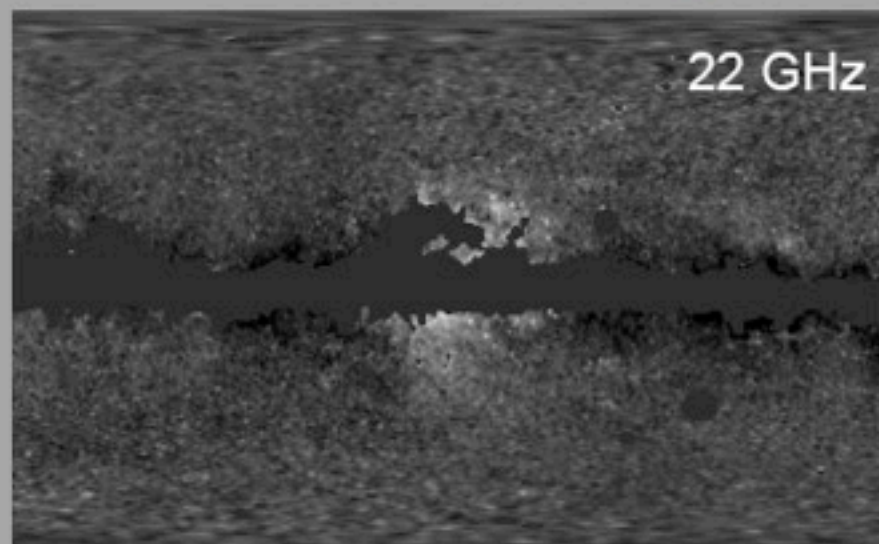
$$\sim 1.2 \times 10^{39} \text{ GeV/sec}$$

2) The total power of the WMAP Haze is between

$$0.7 \times 10^{39} \text{ and } 3 \times 10^{39} \text{ GeV/sec}$$

# Dark Matter in the WMAP Sky

• In 2004, Doug Finkbeiner suggested that the WMAP Haze could be synchrotron from electrons/positrons produced in dark matter annihilations in the inner galaxy (astro-ph/0409027)



• In particular, he noted that:

1) Assuming an NFW profile, a WIMP mass of 100 GeV and an annihilation cross section of  $3 \times 10^{-26} \text{ cm}^3/\text{s}$ , the total power in dark matter annihilations in the inner 2 kpc of the Milky Way is

$\sim 1.2 \times 10^{39} \text{ GeV}/\text{sec}$

**Coincidence?**

2) The total power of the WMAP Haze is between

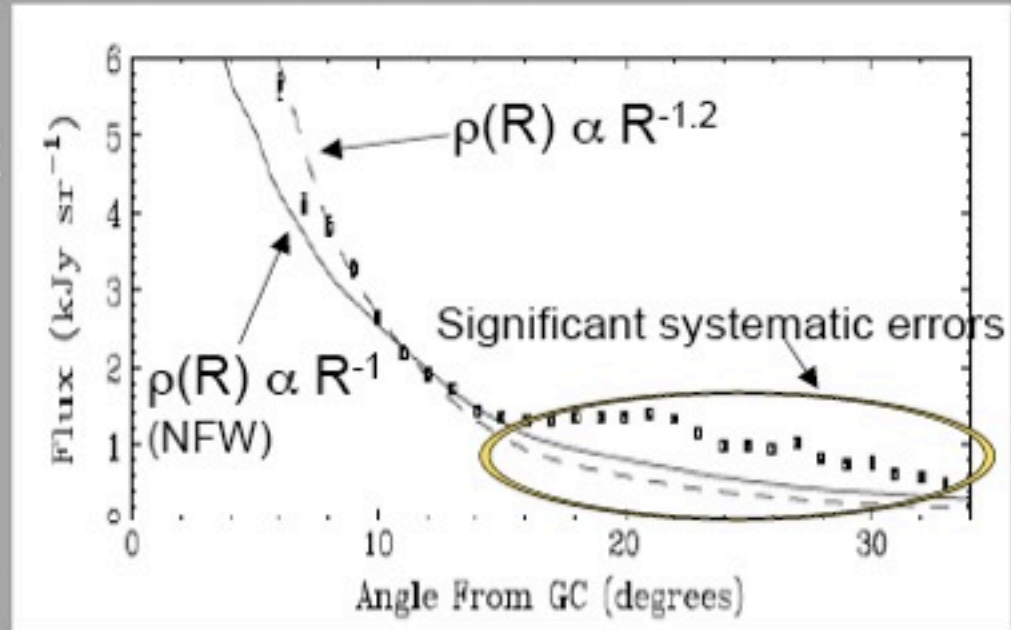
$0.7 \times 10^{39}$  and  $3 \times 10^{39} \text{ GeV}/\text{sec}$

# Fitting The Haze To The Dark Matter Halo Profile

- When the effects of diffusion are accounted for, we find that an NFW halo profile ( $\rho \propto R^{-1}$ ) under produces the WMAP haze at small angles

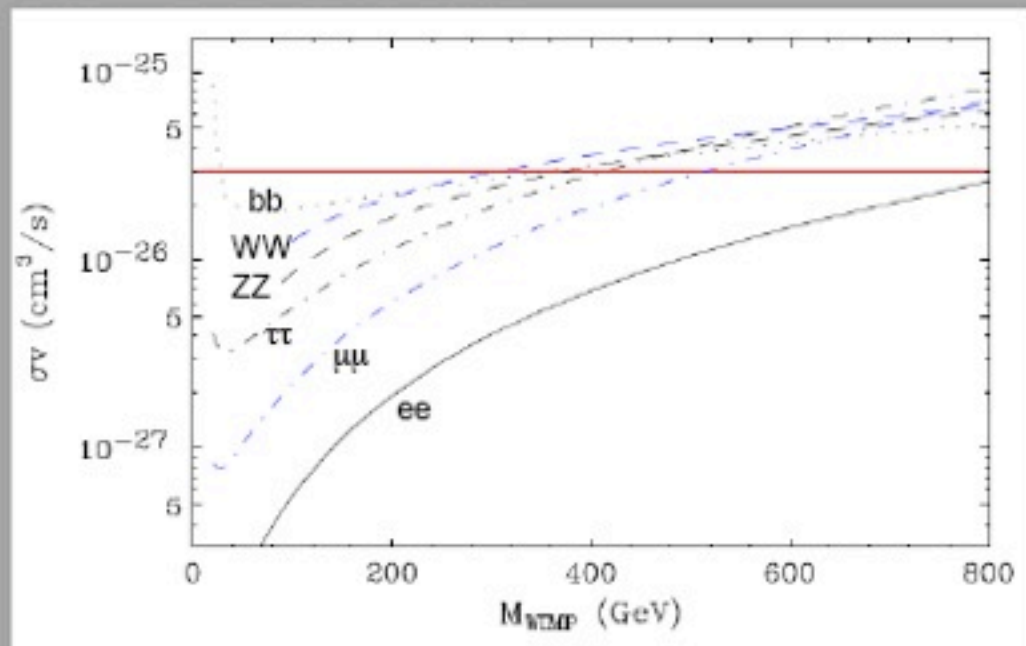
- Angular distribution of the haze matches that found for a profile, with  $\rho \propto R^{-1.2}$

- Although the precise result of this fit depends on the diffusion parameters adopted (magnetic fields, starlight density, etc.), the approximate result (slope of -1.1 to -1.3) is fairly robust



# The Dark Matter Annihilation Cross Section

- For a given annihilation mode, diffusion parameters and halo profile, we can calculate the annihilation cross section needed to normalize to the observed intensity of the WMAP Haze



- For a typical 100-1000 GeV WIMP, the annihilation cross section needed is within a factor of 2-3 of the value needed to generate the density of dark matter thermally ( $3 \times 10^{-26} \text{ cm}^3/\text{s}$ )

- **No boost factors are required!**

# The remarkable match of the WMAP Haze to the signal expected from Dark Matter

The Haze is consistent with dark matter annihilations with the following characteristics:

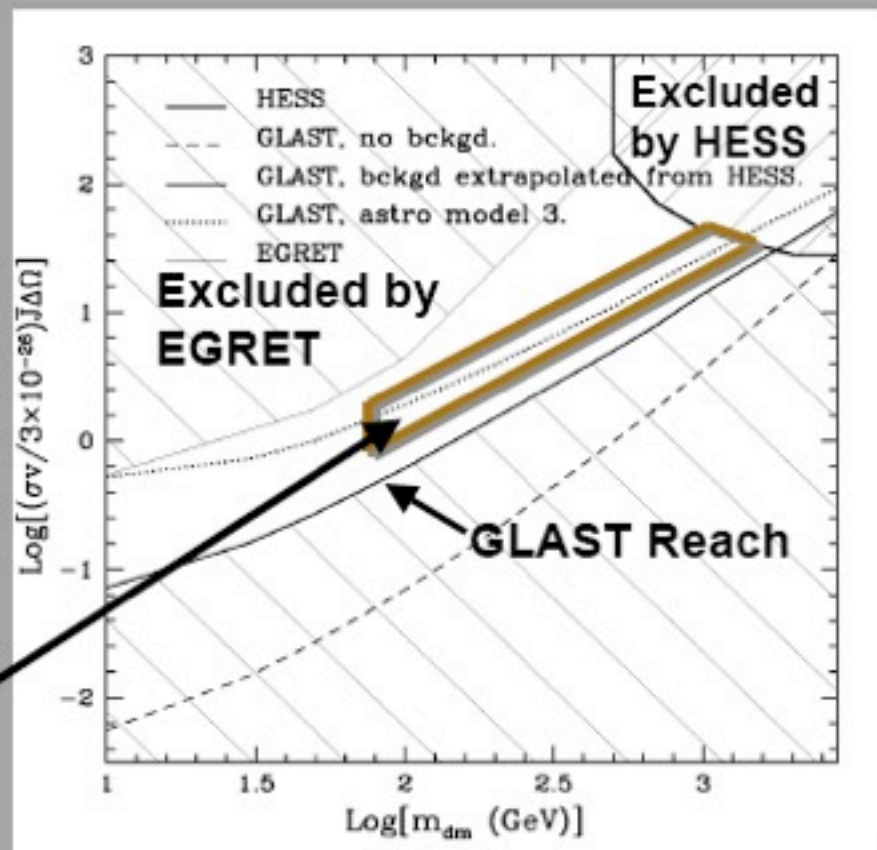
1. A dark matter distribution with  $\rho \propto R^{-1.2}$  in the inner kiloparsecs of our galaxy
2. A dark matter particle with a  $\sim 100$  GeV to several TeV mass, and that annihilates to typical channels (heavy fermions, gauge bosons, etc.)
3. An annihilation cross section within a factor of a few of  $3 \times 10^{-26}$  cm<sup>3</sup>/s (the value required of a thermal relic)

***A completely vanilla dark matter scenario!***

# Gamma-Rays From The Galactic Center

- GLAST will extend the region of the cross section-mass plane excluded by EGRET and HESS considerably
- If we normalize the annihilation rate to that needed to generate the observed intensity of the WMAP Haze, we find that the gamma ray flux is within the reach of GLAST

**Range Predicted By  
the WMAP Haze**



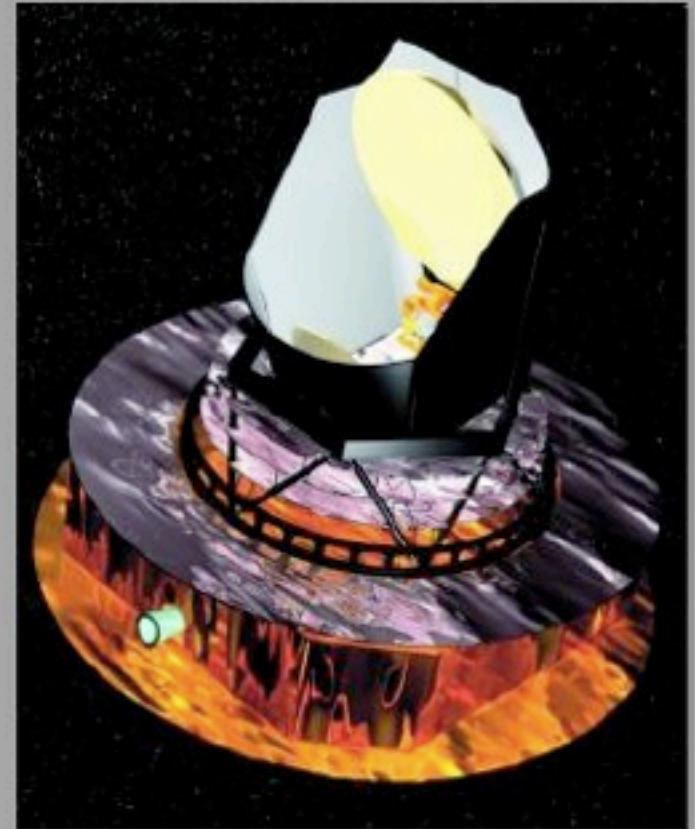
# The WMAP Haze In Light Of Planck

Planck (launch in 2008) will represent a major step forward from WMAP:

- Improved frequency coverage
- Improved angular resolution

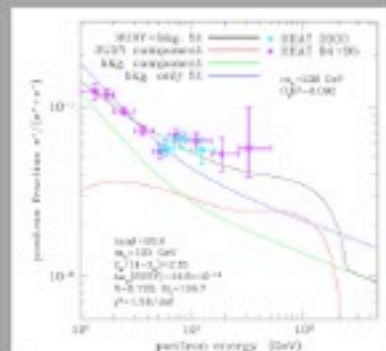
- At frequencies above  $\sim 100$  GHz, all foregrounds other than emission from thermal dust are negligible; subtracting one foreground rather than the several (3 or 4) required at WMAP frequencies will enable for a much more robust confirmation of the hard synchrotron origin of the Haze

- Systematic uncertainties are expected to be reduced by more than an order of magnitude relative to WMAP

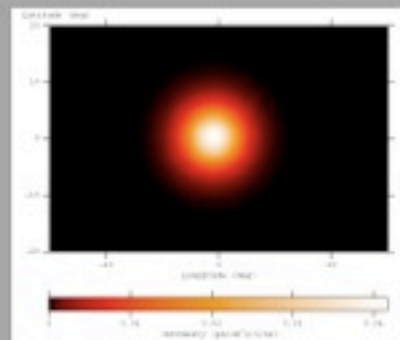


# What About Other Claims of Evidence For Dark Matter Annihilation?

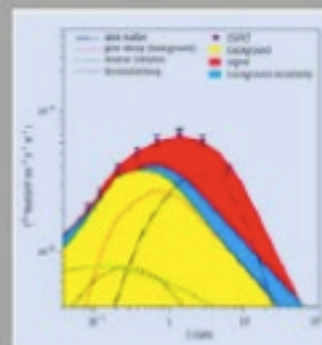
- The HEAT positron excess



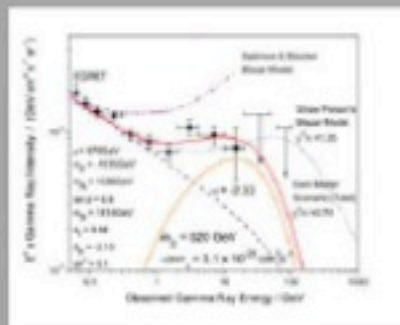
- 511 keV emission from the galactic bulge



- EGRET's galactic gamma ray spectrum



- EGRET's extragalactic gamma ray spectrum



Signal	Required Particle Physics	Required Astrophysics
WMAP Haze	100 GeV to multi-TeV WIMP, $\sim 3 \times 10^{-26}$ cm <sup>3</sup> /s annihilation cross section	Cusped halo profile, standard diffusion, no boost factors
HEAT Positron Excess	50-1000 GeV WIMP; Either large (non-thermal) annihilation cross section OR ...	Large boost factor (50 or more)
INTEGRAL 511 keV Emission	$\sim$ MeV particle, p-wave annihilator with $\sim 3 \times 10^{-26}$ cm <sup>3</sup> /s annihilation cross section	Mildly cusped halo profile
EGRET Diffuse Galactic	$\sim$ 50-300 GeV WIMP; Either large (non-thermal) annihilation cross section OR ...	Large boost factors; two massive rings of dark matter in the galactic plane; non-standard, highly convective diffusion model
EGRET Diffuse Extragalactic	$\sim$ 500 GeV WIMP; Either large (non-thermal) annihilation cross section OR ...	Large boost factors/highly cusped profiles; Conflict with Milky Way unless Galactic Center is exceptional

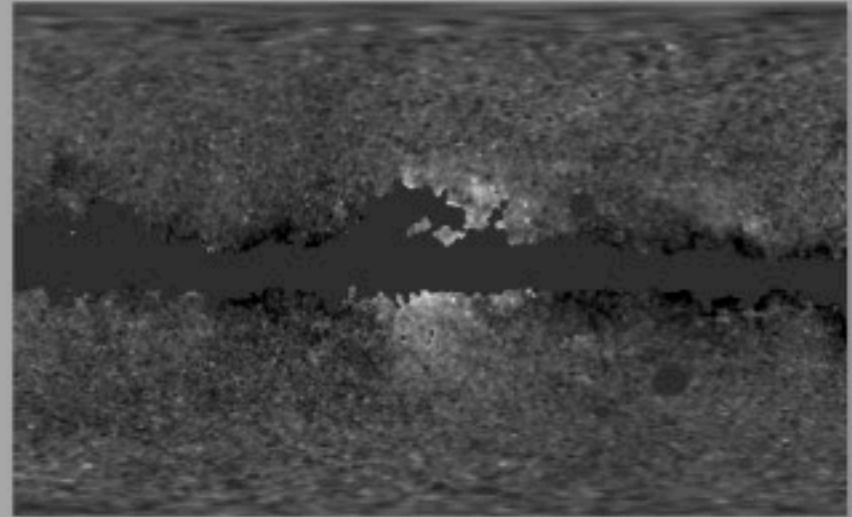
Signal	Required Particle Physics	Required Astrophysics
WMAP Haze	100 GeV to multi-TeV WIMP, $\sim 3 \times 10^{-26}$ cm <sup>3</sup> /s annihilation cross section	Cusped halo profile, standard diffusion, no boost factors
HEAT Positron Excess	50-1000 GeV WIMP; Either large (non-thermal) annihilation cross section OR ...	Large boost factor (50 or more)
INTEGRAL 511 keV Emission	$\sim$ MeV particle, low wave annihilator with $\sim 3 \times 10^{-26}$ cm <sup>3</sup> /s annihilation cross section	Mildly cusped halo profile
EGRET Diffuse Galactic	$\sim$ 50-300 GeV WIMP; Either large (non-thermal) annihilation cross section OR ...	Large boost factors; two massive rings of dark matter in the galactic plane; non-standard, highly convective diffusion model
EGRET Diffuse Extragalactic	$\sim$ 500 GeV WIMP; Either large (non-thermal) annihilation cross section OR ...	Large boost factors/highly cusped profiles; Conflict with Milky Way unless Galactic Center is exceptional

# Conclusions

- WMAP data, after the subtraction of known foregrounds, contains an excess from the region around the center of the Milky Way - The “WMAP Haze”

- Consistent with synchrotron emission from energetic electrons/positrons from dark matter annihilations with:

- A cusped halo profile
- A 100-1000 GeV WIMP
- An annihilation cross section within a factor of 2-3 of the value required of a thermal relic ( $\sim 3 \times 10^{-26} \text{ cm}^3/\text{s}$ )



***A completely vanilla dark matter scenario!***

[Here's why I said not to take the previous slides too seriously!]

# Dark Matter in the WMAP Sky?

## Seven-Year Wilkinson Microwave Anisotropy Probe (WMAP) Observations: Galactic Foreground Emission

B. Gold<sup>2</sup>, N. Odegard<sup>3</sup>, J. L. Weiland<sup>3</sup>, R. S. Hill<sup>3</sup>, A. Kogut<sup>4</sup>, C. L. Bennett<sup>2</sup>, G. Hinshaw<sup>4</sup>, X. Chen<sup>5</sup>, J. Dunkley<sup>6</sup>, M. Halpern<sup>7</sup>, N. Jarosik<sup>8</sup>, E. Komatsu<sup>9</sup>, D. Larson<sup>2</sup>, M. Limon<sup>10</sup>, S. S. Meyer<sup>11</sup>, M. R. Nolta<sup>12</sup>, L. Page<sup>8</sup>, K. M. Smith<sup>13</sup>, D. N. Spergel<sup>8;13</sup>, G. S. Tucker<sup>14</sup>, E. Wollack<sup>4</sup>, and E. L. Wright<sup>5</sup>

29 January 2010

### *From the Abstract:*

We present updated estimates of Galactic foreground emission using seven years of WMAP data. Using the power spectrum of differences between multifrequency template-cleaned maps, we find no evidence for foreground contamination outside of the updated (KQ85y7) foreground mask. We place a 15  $\mu\text{K}$  upper bound on rms foreground contamination in the cleaned maps used for cosmological analysis. Further, the cleaning process requires only three power-law foregrounds outside of the mask. We find no evidence for polarized foregrounds beyond those from soft (steep-spectrum) synchrotron and thermal dust emission; in particular **we find no indication in the polarization data of an extra "haze" of hard synchrotron emission from energetic electrons near the Galactic center.**

# Dark Matter in the WMAP Sky?

Seven-Year Wilkinson Microwave Anisotropy Probe (WMAP) Observations:  
Galactic Foreground Emission - B. Gold et al. 29 January 2010

## 4.5. The Haze

In its low frequency bands, WMAP observes an excess of emission above what was predicted by scaling the 408 MHz to higher frequencies using the expected spectral index for synchrotron emission. Determining the exact nature of this emission has proven difficult; WMAP has generally treated it as a hard (flatter spectrum) synchrotron component without attempting to explain the origin of such a component. Other suggestions have involved combinations of different types of spinning dust (Finkbeiner 2004; Dobler & Finkbeiner 2008b), though there is typically still a residual “haze” even after those components are fit out (Dobler & Finkbeiner 2008a).

It has been argued that this remainder low-frequency emission has an ellipsoidal shape and is consistent with hard synchrotron emission, possibly from dark matter annihilation in the core of the Galaxy (Hooper et al. 2007). There has been tentative detection of a haze in gamma-rays using preliminary data from the Fermi telescope (Dobler et al. 2009).

Interpretation of polarization information toward the center of the Galaxy is difficult, as depolarization through line-of-sight changes in the orientation of the magnetic field can affect the signal significantly. Nonetheless, we search for a hard component in the polarization data using a simplified version of the low-resolution MCMC fit of Dunkley et al. (2009a), shown in Figure 7. We do not detect any significant change of synchrotron spectral index as a function of Galactocentric distance.

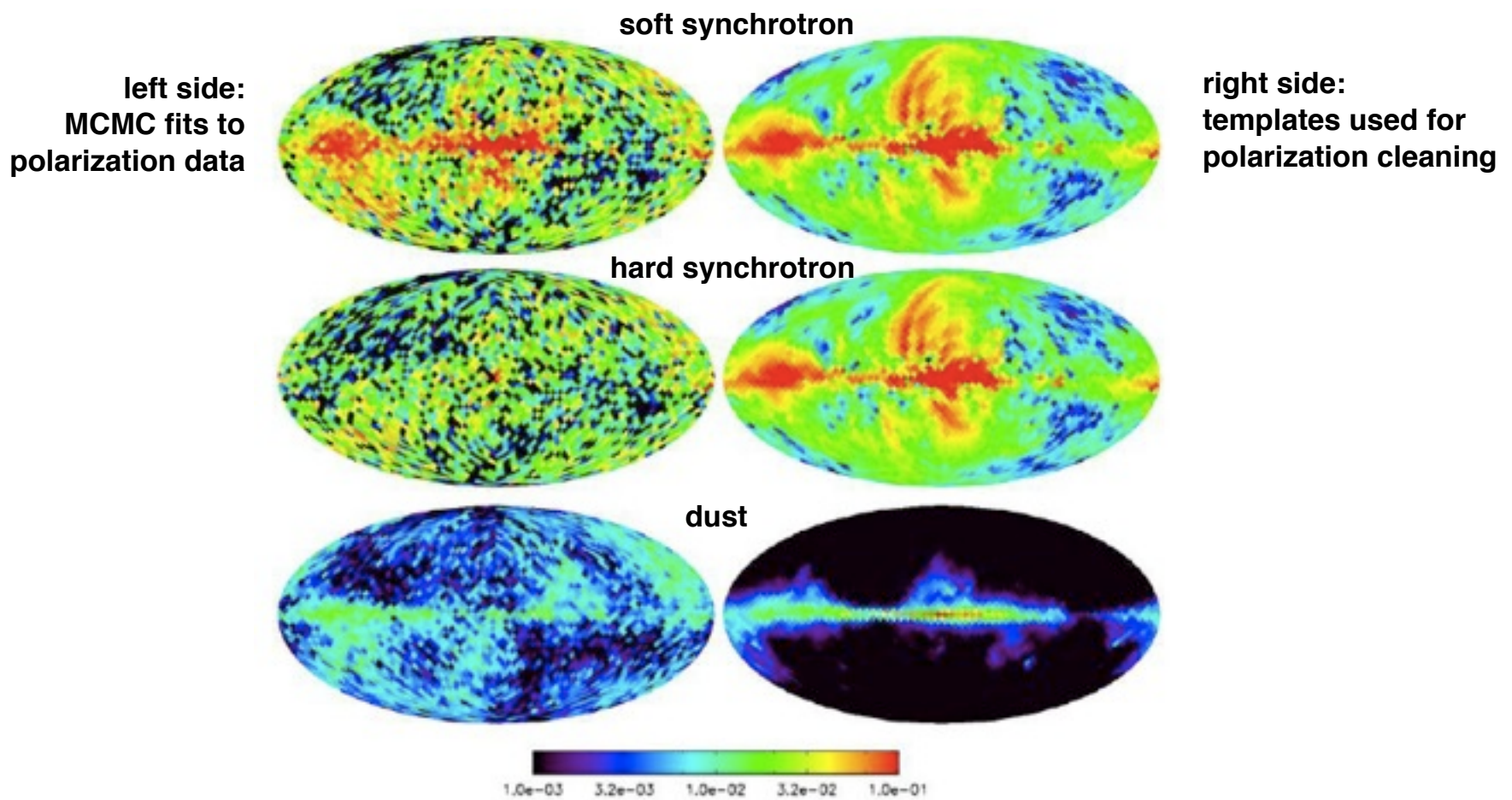


**Fig. 7. Comparison of the templates used for polarization cleaning to a low-resolution ( $N_{\text{side}} = 16$ ) MCMC fit to polarization data using a three-component model with fixed spectral indexes to search for any hard synchrotron component. The left column shows the results of the MCMC fit to polarization data using three components: soft synchrotron at top, hard synchrotron at middle, and dust at bottom. For comparison, the right column shows the templates used for polarization cleaning: synchrotron at top and middle, and dust and bottom. All plots are of polarization intensity  $P$  with a logarithmic scale from 1 to 100  $\mu\text{K}$ . Synchrotron intensity is measured at a reference frequency of 23 GHz, and dust intensity at 94 GHz. The MCMC maps are noisy, and have been corrected for a noise bias in  $P$  caused by noise in  $Q$  and  $U$ . Excess noise in the plane of the ecliptic due to the scan pattern is also clearly visible in the MCMC fits. Given the noise level, hard synchrotron emission does not appear to be significant.**

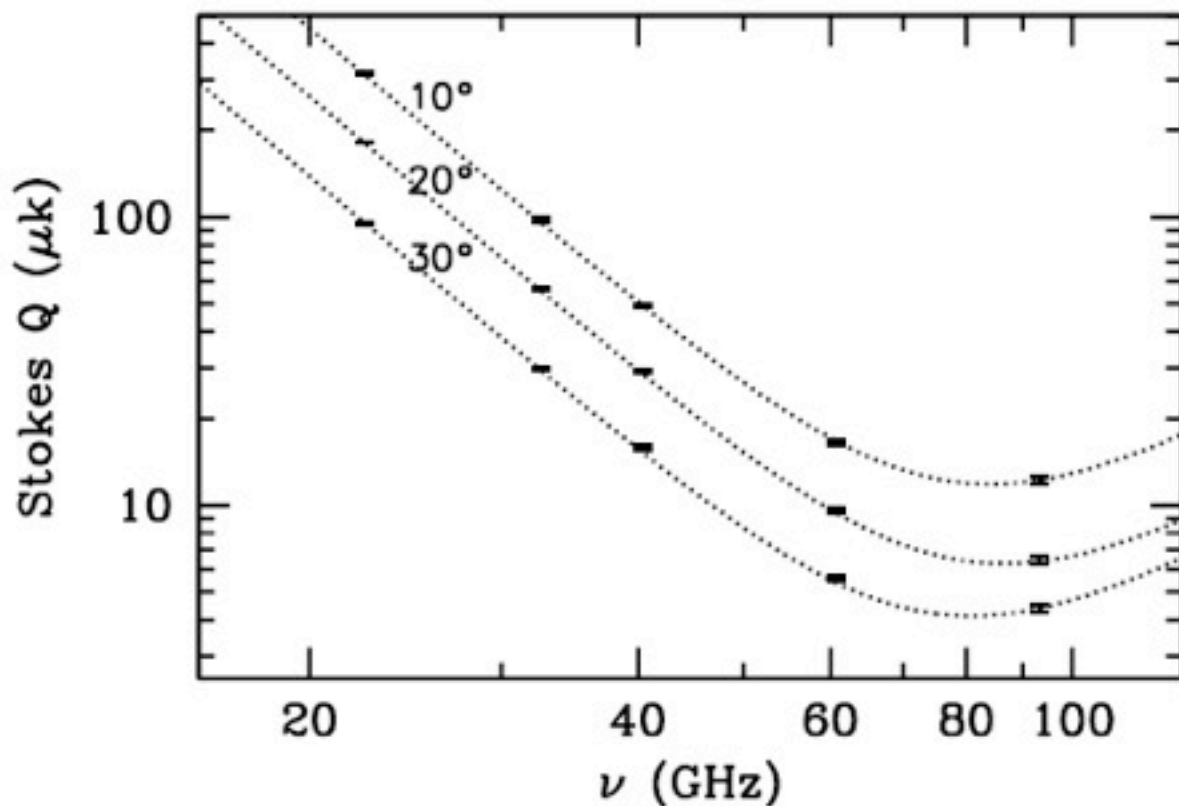


Fig. 8.— Frequency spectrum of polarized emission around the Galactic center. Average antenna temperature of Stokes Q is shown for three oval regions defined by  $\sqrt{l^2 + (2b)^2} < 10^\circ, 20^\circ, 30^\circ$ , where  $l$  and  $b$  are Galactic longitude and latitude. Stokes U is negligible at all frequencies except W-band. Errorbars indicate statistical uncertainty from the diagonal part of the pixel-pixel noise matrix. Dotted lines show the sum of a synchrotron component with  $\beta = -3.2$  and a dust component with  $\beta = +2.0$ ; in all cases this two-component model is sufficient to explain the observations.

This special fit was done at HEALPix  $N_{\text{side}} = 16$  using *only WMAP* polarization data, so as to be insensitive to any uncertainties regarding the presence or absence of spinning dust. The fit attempts to model the sky as a sum of three power-law foregrounds: a soft synchrotron component with  $\beta = -3.1$ , a hard synchrotron component with  $\beta = -2.39$ , and a dust component with  $\beta = +2.0$ . These power-law indices were those suggested by the work of Dobler & Finkbeiner (2008a).

The results of the fit are shown in Figure 7. Residuals after the fit are small compared to the noise, and over all bands the mean reduced  $\chi^2$  per pixel is 1.1. For comparison, the synchrotron and dust templates used for polarization cleaning are shown in the right column of the figure. The MCMC result for the soft synchrotron template appears to be essentially a noisy version of the synchrotron template, indicating that K-band indeed is a good proxy for polarized synchrotron emission. For dust, the MCMC and template results differ somewhat. The MCMC hard synchrotron results show no spatial structure beyond *WMAP*'s noise pattern, and are consistent with the level of noise bias expected in a map of  $P = \sqrt{Q^2 + U^2}$ .

Figure 8 shows the frequency spectrum of polarized emission for elliptical regions around the Galactic center. In these regions the polarization direction is nearly vertical, and so the Stokes U parameter is negligible for bands K through V and small for W-band. The spectra for three different regions are shown, sized  $10^\circ \times 5^\circ$ ,  $20^\circ \times 10^\circ$ , and  $30^\circ \times 15^\circ$ . We find no evidence for emission other than soft synchrotron ( $\beta = -3.2$ ) and dust ( $\beta = +2.0$ ), in particular, no “haze” component appears to be necessary for polarization.

# Axion Physics in a Nutshell

**Why axions?** QCD with  $m_{\text{quarks}} \neq 0$  violates **CP** and therefore **T** due to instantons, unless an undetermined parameter  $\theta$  is very small – or the axion field absorbs the **CP**-violating phase. If this **CP** violation isn't avoided, the neutron gets an electric dipole moment  $10^{10}$  times larger than the experimental upper bound!



**When** the temperature  $T$  drops to  $T \sim f_a$ , the axion field gets a vacuum expectation value  $f_a e^{i\theta}$ , and then when  $T$  drops to  $\Lambda_{\text{QCD}} \sim 100 \text{ MeV}$  QCD causes the axion to get mass  $m_a$  and density  $\rho_a \propto 1/m_a$ .

**What?** Axions are never relativistic, so there is no free streaming to erase fluctuations in their density. So they behave like Cold Dark Matter.

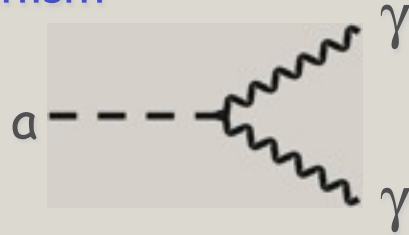
# Axion Physics in a Nutshell

## Particle-Physics Motivation

CP conservation in QCD by Peccei-Quinn mechanism

→ Axions  $a \sim \pi^0$

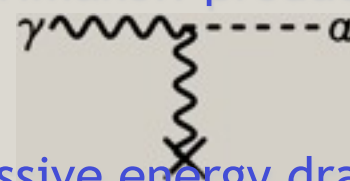
$$m_\pi f_\pi \approx m_a f_a$$



For  $f_a \gg f_\pi$  axions are “invisible” and very light

## Solar and Stellar Axions

Axions thermally produced in stars, e.g. by Primakoff production



• No excessive energy drain:

$$m_a < 10 \text{ meV}$$

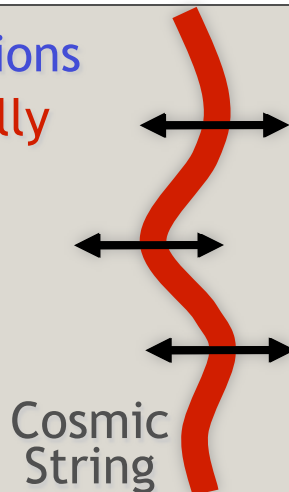
• Search for solar axions (CAST)

## Cosmology

In spite of small mass, axions are born **non-relativistically** (“non-thermal relics”)

→ “Cold dark matter” candidate

$$m_a \sim 1\text{-}1000 \text{ } \mu\text{eV}$$



## Search for Axion Dark Matter



Microwave resonator  
(1 GHz = 4  $\mu\text{eV}$ )



# Experimental Search for Axions

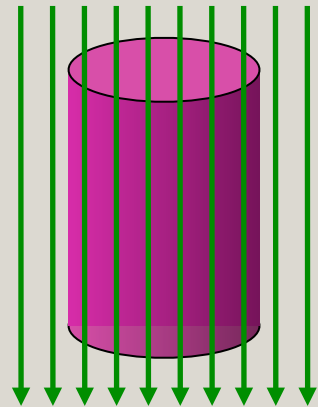
DM axions  
Velocities in  
galaxy

$$m_a = 10\text{-}3000$$
$$\mu\text{eV}$$
$$v_a \approx 10^{-3} c$$



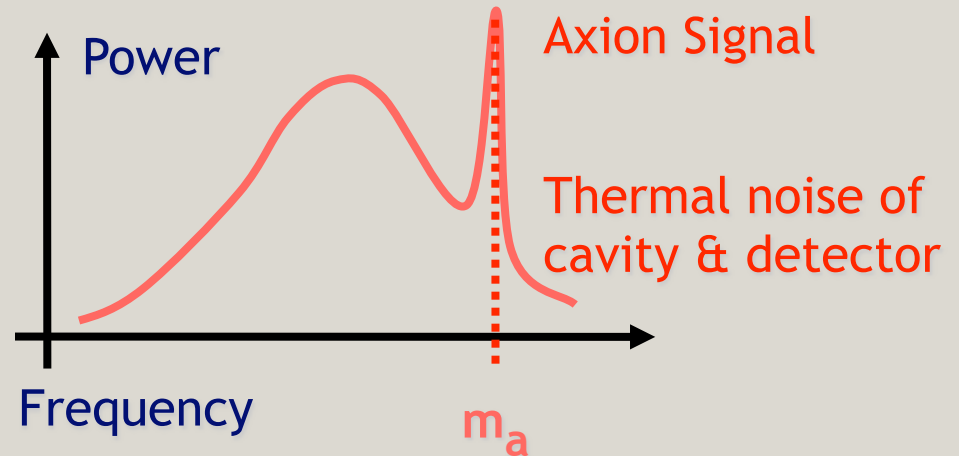
Microwave Energies  
(1 GHz  $\approx$  4  $\mu\text{eV}$ )

## Axion Haloscope (Sikivie 1983)



$$B_{\text{ext}} \approx 8 \text{ Tesla}$$

Microwave  
Resonator  
 $Q \approx 10^5$



## Primakoff Conversion



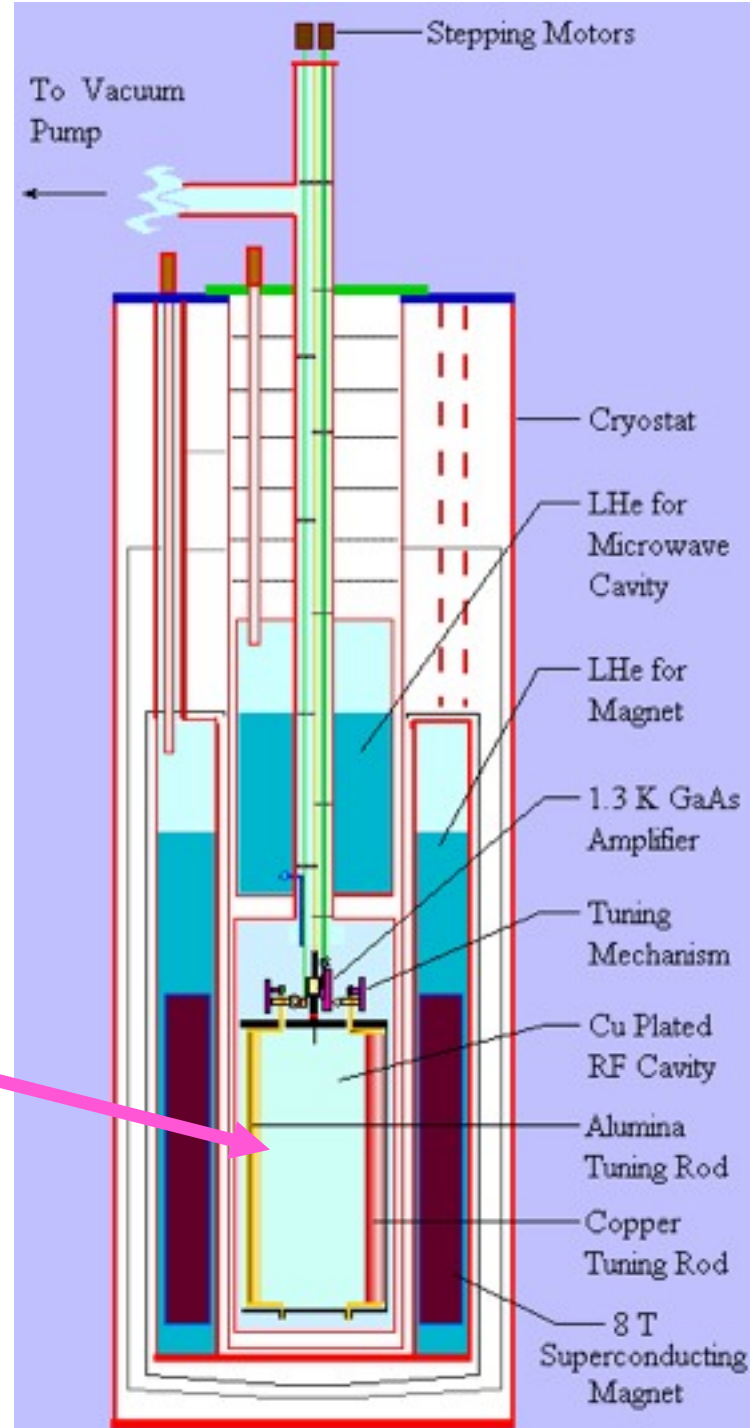
## 2 Experiments in Operation

- Axion Dark Matter Experiment (ADMX), Livermore, US
- CARRACK II, Kyoto, Japan

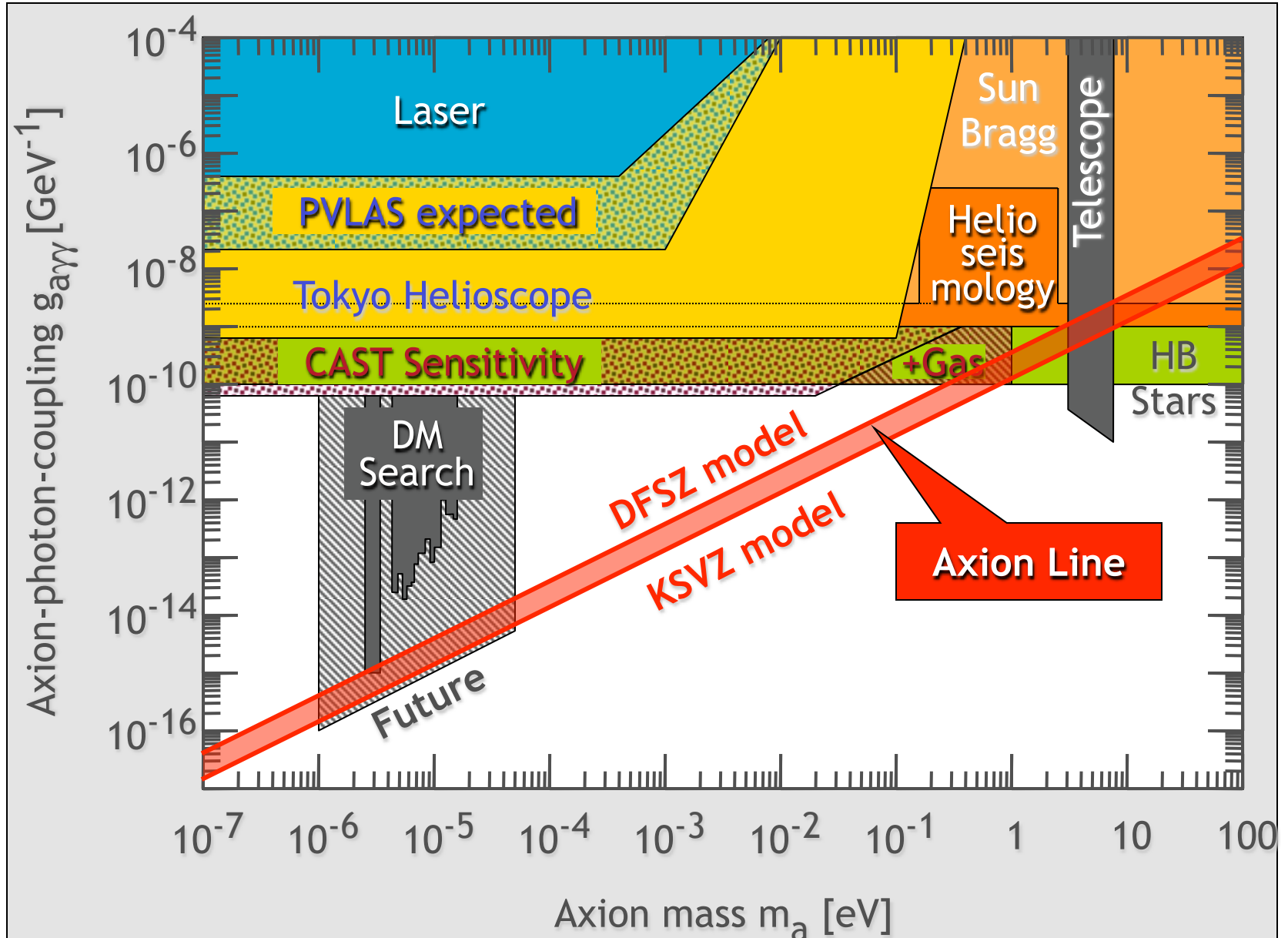
# AXION search

The diagram at right shows the layout of the axion search experiment now underway at the Lawrence Livermore National Laboratory. Axions would be detected as extra photons in the Microwave Cavity.

An improved version of this experiment is moving to the University of Washington.



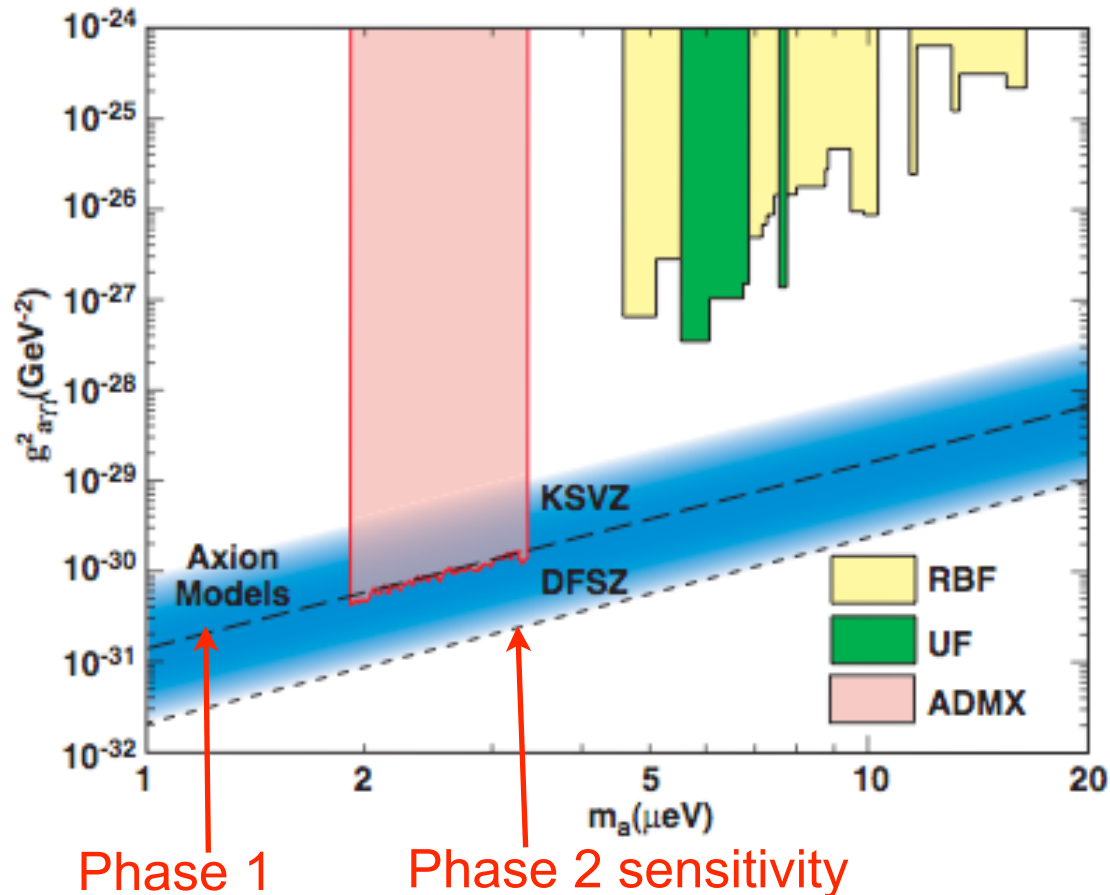
# Limits on Axion-Photon-Coupling



# AXION search

**The Strong CP Problem.** The standard SU(3) theory of the Strong force violates CP conservation, for example predicting that the neutron has an electric dipole moment  $10^8$  times bigger than the current upper limit, unless an uncalculable parameter is very small. The only elegant solution to this "Strong CP Problem" involves a new particle that interacts so weakly that it has never been detected before. This particle is the Axion. Fortunately this particle would interact with other particles just enough that if you went looking for it very carefully, you might be able to find it.

The **Axion DM Experiment (ADMX)** is designed to look into only a slice of the allowed mass range. The reason it's only a slice and not the whole range is simply due to the equipment. The frequency that is scanned by ADMX depends on the tuning rods and the resonant cavity. Making the apparatus able to scan a larger frequency range would have cost more and made the apparatus bigger, which makes cooling and transportation harder, among other things. As to why it is that particular slice, it's because it's the most convenient one to look in. There's no significant reason to believe that the Axion would be more likely to be in any particular range, so this one was chosen based on it being easiest to scan with current technology.



# Axion Dark Matter Summary for KISS Dark Matter Workshop

Joel Primack, UCSC

## Relation between axion mass, PQ symmetry breaking scale, and e-m coupling

Following the axion physics reviews by Mike Turner and George Raffelt [1], the relation between the axion mass  $m_a$  and the Peccei-Quinn (PQ) symmetry breaking energy scale  $f_{PQ}$  is

$$m_a = z^{1/2} (1+z)^{-1} f_\pi m_\pi / (f_{PQ}/N) \approx 6.0 \mu\text{eV } F^{-1}, \text{ or } F \approx 6.0 \mu\text{eV} / m_a . \quad (1)$$

Here  $z = m_u/m_d \approx 0.56$  is the ratio of up and down quark masses (which Raffelt [1] notes could lie between 0.3 and 0.6),  $m_\pi = 135 \text{ MeV}$ ,  $f_\pi = 95 \text{ MeV}$ , and  $N$  is the color anomaly of the PQ symmetry (a model-dependent quantity), and we define

$$F \equiv (f_{PQ}/N)/10^{12} \text{ GeV}. \quad (2)$$

To further clarify the role of  $f_{PQ}/N$ , the axion field  $a = (f_{PQ}/N) \theta$ , where  $\theta$  appears as

$$\mathcal{L}_{\text{QCD}} = \mathcal{L}_{\text{pert.}} + \theta \left( g^2/32\pi^2 \right) G_{\mu\nu a} \tilde{G}^{\mu\nu a}, \quad (3)$$

multiplying the non-perturbative CP-violating term in the QCD Lagrangian. The coupling  $g_{a\gamma\gamma}$  between the axion field and the electromagnetic field in the interaction Lagrangian is

$$\mathcal{L}_{\text{int}} = \dots - g_{a\gamma\gamma} a \mathbf{E} \cdot \mathbf{B} . \quad (4)$$

Here

$$g_{a\gamma\gamma} = (\alpha/2\pi) (N/f_{PQ}) [E/N - (2/3)(4+z)/(1+z)] , \quad (5)$$

$\alpha = 1/137$  is the fine structure constant, and  $E$  is the PQ electromagnetic anomaly, which depends on the model-dependant  $u, d$  quark and electron PQ charges  $X_i$ , where  $i = u, d, e$ . If  $X_e = 0$  the axion is hadronic (the KSVZ model), while in the DFSZ model  $X_e \neq 0$ . Then

$$g_{a\gamma\gamma} = (m_a/6.2 \mu\text{eV}) (\alpha/2\pi) [E/N - (2/3)(4+z)/(1+z)]/(10^{12} \text{ GeV}) . \quad (6)$$

In the simplest GUTs and in DFSZ,  $E = 8/3$  and  $[E/N - (2/3)(4+z)/(1+z)] \approx 0.72$ , and

$$g_{a\gamma\gamma} = (m_a/\mu\text{eV})/(7.4 \times 10^{15} \text{ GeV}). \quad (7)$$

$E/N=0$  for the KSVZ model. It is possible for the factor in brackets [...] to nearly vanish in other models. In the Figure summarizing the current constraints on axion mass and  $g_{a\gamma\gamma}$  at the end of these notes, the DFSZ line corresponds to  $g_{a\gamma\gamma} \approx (m_a/\mu\text{eV})/(10^{16} \text{ GeV})$  and the KSVZ line corresponds to  $g_{a\gamma\gamma} \approx 4(m_a/\mu\text{eV})/(10^{16} \text{ GeV})$ .

## Axion contribution to dark matter density $\Omega_a$

**Thermal axions.** If the axion is hadronic, there is an allowed mass window roughly 2 - 10 eV (which is excluded by red giants if  $X_e \neq 0$ ). In this case, axions couple strongly enough to be produced thermally in the early universe, with  $\Omega_a \sim 10^{-2} h^{-2} (m_a/\text{eV})$ . Searches for lines from axion decay to two photons with wavelength  $\lambda_a = 2hc/m_a = 24,800\text{\AA}/(m_a/\text{eV})$  have ruled this out for  $4.5 \text{ eV} < m_a < 7.7 \text{ eV}$  unless [...]  $\approx 0$  [2].

**Cold axions.** Regarding  $\Omega_a$  from cold axions, there are two cases to consider, depending on when PQ symmetry breaks:

**(case 1)** PQ symmetry breaks after inflation ends, so that the universe is filled with domains of horizon size when PQ-breaking occurs, each with different values of the initial misalignment angle  $\theta_0$ , which eventually results in  $\theta_0$  averaging to  $\theta_0 = \pi/\sqrt{3} = 1.814$ . In this case, Sikivie's 2008 review [3] says that

$$\Omega_a = 0.7 (h/0.7)^2 F^{7/6} . \quad (8)$$

Thus  $\Omega_a = \Omega_{\text{CDM}} = 0.23$  if the cold dark matter is axions, or  $\Omega_a < 0.23$  if axions contribute only part of the dark matter. Taking  $h=0.7$ , we find  $F < 0.39$ , and

$$m_a = 6 \mu\text{eV} (\Omega_a/0.7)^{6/7} = 2.3 \mu\text{eV} (\Omega_a/0.23)^{6/7} . \quad (9)$$

$$m_a = 6 \mu\text{eV} (\Omega_a/0.7)^{6/7} = 2.3 \mu\text{eV} (\Omega_a/0.23)^{6/7} . \quad (9)$$

However, the result in eq. (9) has been controversial, as different authors (e.g. [4]) have disagreed with Sikivie regarding the relative contribution to  $\Omega_a$  of the decay of the network of axion strings producing axions compared to the "axion sloshing" mode. A recent email from O. Wantz of E. P. S. Shellard's group says that their calculations (paper in preparation) would replace 2.3  $\mu\text{eV}$  in eq. (9) by 70  $\mu\text{eV}$ , with an uncertainty of about a factor of 2 or 3.

Also, a recent paper by Sikivie and Yang [5] claims that the cold axions form a Bose-Einstein condensate (BEC), which would lead to a large integrated Sachs-Wolfe (ISW) effect, with uncertain implications for constraints on this scenario.

**(case 2)** PQ symmetry breaks before inflation ends, and the entire observable universe has the same value of  $\theta_0$ . In that case, there is the uncontroversial result (e.g., [3] eq. 101; [6], eq. 6)

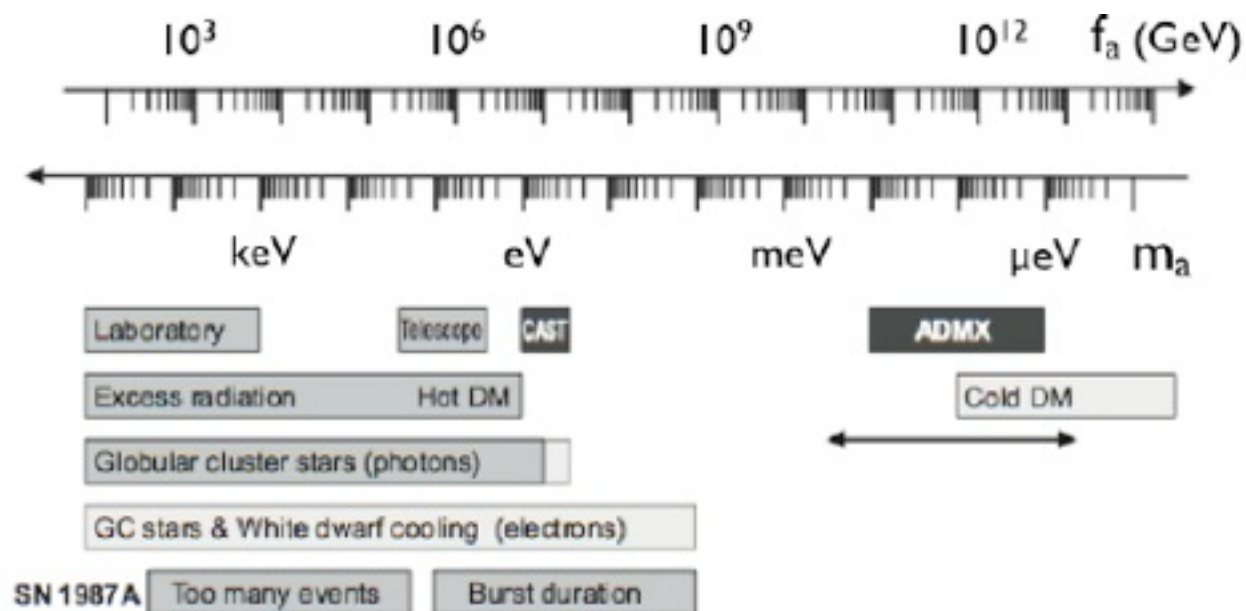
$$\Omega_a = 0.15 (h/0.7)^2 F^{7/6} \theta_0^2 . \quad (10)$$

Correspondingly, the lower limit of  $\sim 1 \mu\text{eV}$  on  $m_a$  is decreased if  $\theta_0$  happens to be small:

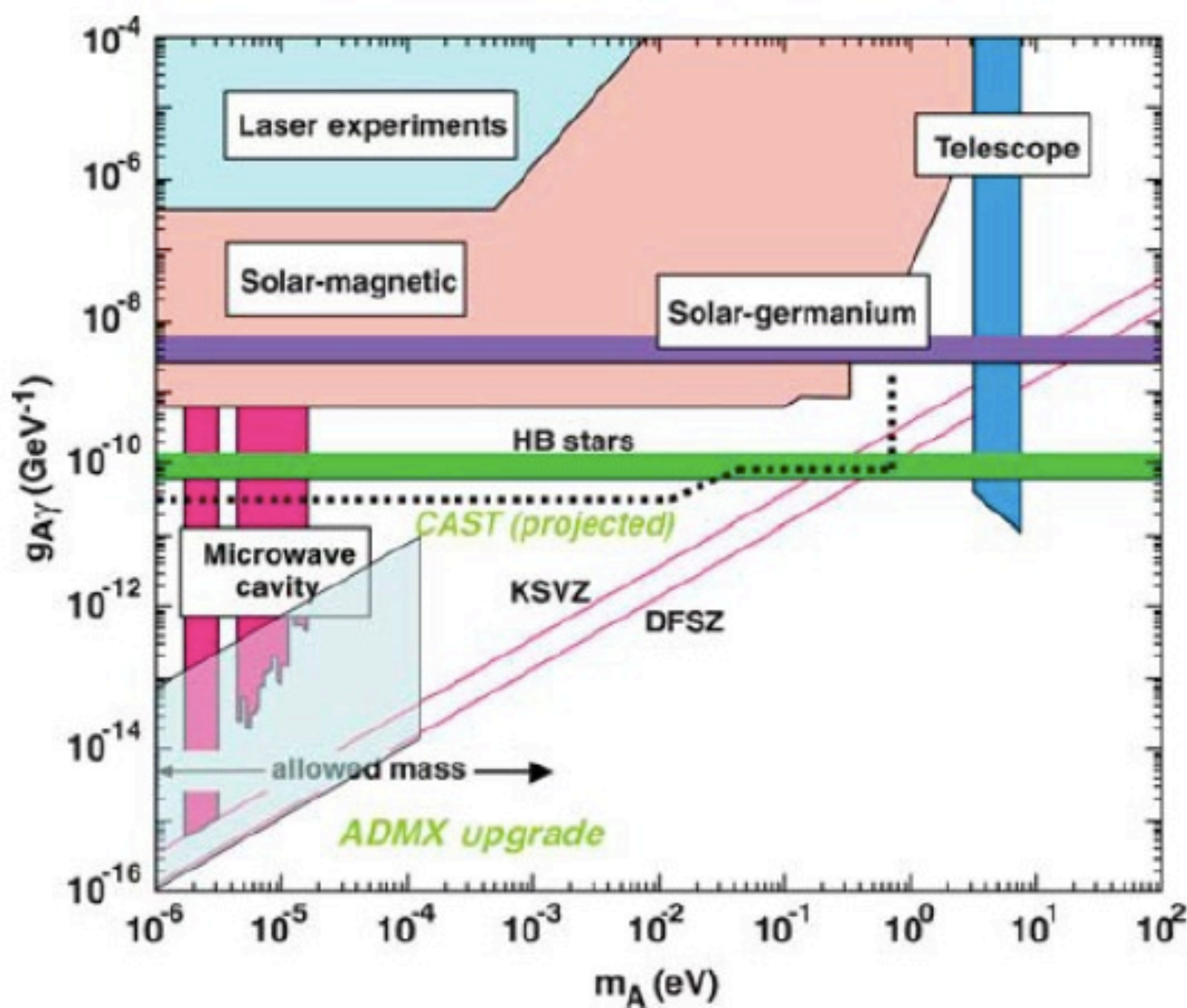
$$m_a = 8.7 \mu\text{eV} (\Omega_a/0.23)^{6/7} \theta_0^{12/7} . \quad (11)$$

There is an additional constraint in this case, since if  $F$  is too large, corresponding to  $\theta_0 \ll 1$  and  $m_a \ll 1 \mu\text{eV}$ ,  $f_{\text{PQ}}$  becomes larger than the GUT scale and/or isocurvature fluctuations become larger than 10% in  $P(k)$  and incompatible with observational constraints favoring adiabatic fluctuations. (This is reviewed in Section 6 of [3].)

Note that the upgraded Livermore-University of Washington cavity axion search experiment ADMX is mainly sensitive to  $m_a \sim 1 - 10 \mu\text{eV}$ , although the Figure below suggests that it could cover the range up to about  $100 \mu\text{eV}$ . Melissinos [7] recently proposed an optical cavity method that is claimed to cover the range  $m_a = 1 - 100 \mu\text{eV}$ .



Astrophysical and cosmological constraints on axions. Light grey exclusion bars are very model dependant. The black bars are the CAST and ADMX search ranges. (From Raffelt [1].)



Axion two-photon coupling  $g_{a\gamma\gamma}$  versus  $m_a$ , with all experimental and observational constraints. ADMX: Axion Dark Matter eXperiment; CAST: CERN Axion Telescope; HB stars: horizontal-branch stars. (From [8].)

## Caustics

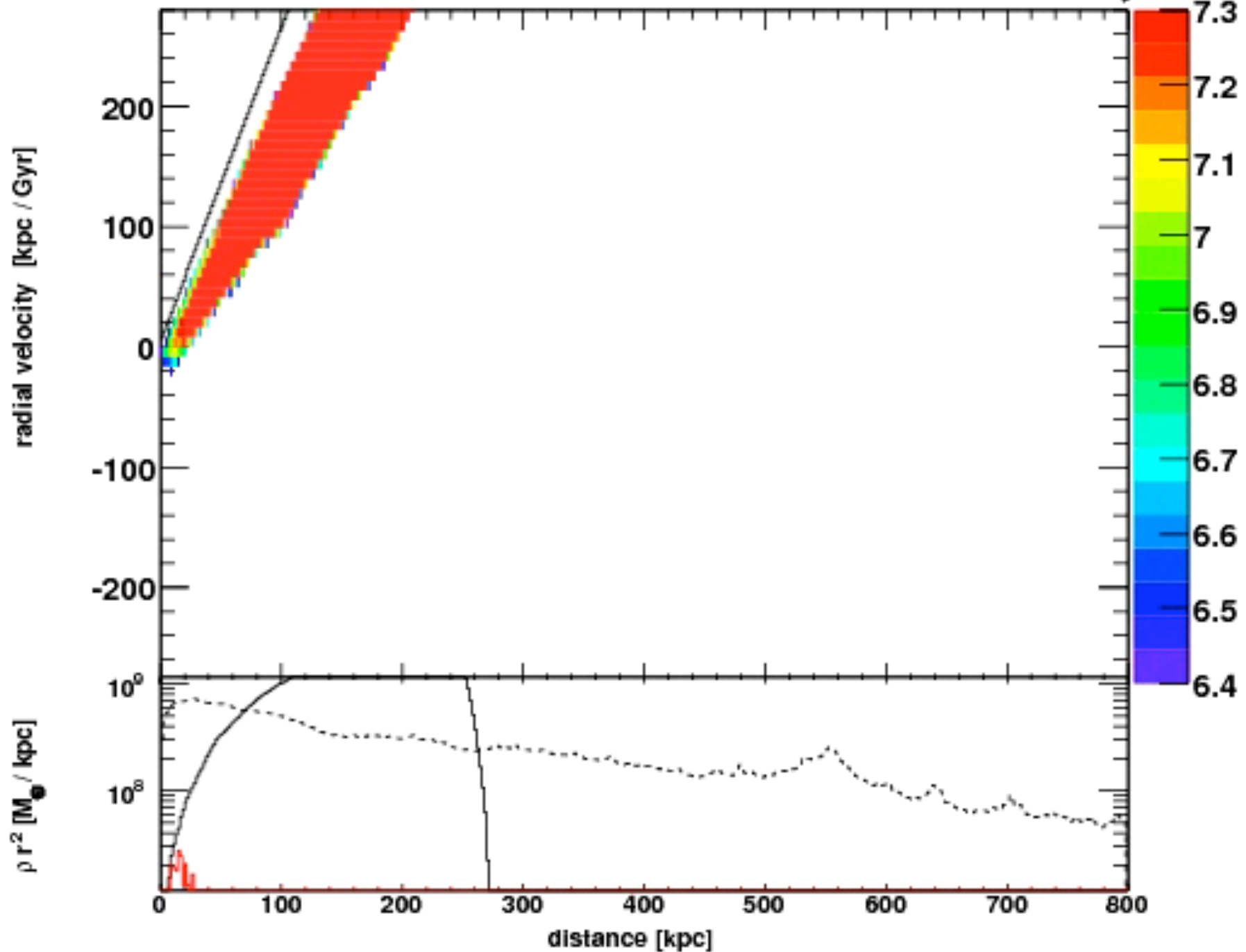
Sikivie and collaborators [9] have argued that infall of dark matter onto the Milky Way will give rise to strong dark matter caustics at the solar radius, which could give rise to signals in a high-resolution axion cavity detector. However, these arguments are based on unphysical assumptions that are strongly ruled out by modern simulations, e.g. [10]. If the cold axions are a Bose-Einstein Condensate [5], such caustics are not expected.

### Infall Caustics in Dark Matter Halos?

Jürg Diemand & Michael Kuhlen, *ApJ Letters* 680, L25 (2008)

We show that most particle and subhalo orbits in simulated cosmological cold dark matter halos are surprisingly regular and periodic: the phase-space structure of the outer halo regions shares some of the properties of the classical self-similar secondary infall model. Some of the outer branches are clearly visible in the radial velocity-radius plane at certain epochs. However, they are severely broadened in realistic, triaxial halos with nonradial, clumpy, mass accretion. This prevents the formation of high-density caustics: even in the best cases there are only broad, very small (<10%) enhancements in the spherical density profile. Larger fluctuations in  $\rho(r)$  caused by massive satellites are common. Infall caustics are therefore too weak to affect lensing or dark matter annihilation experiments. Their detection is extremely challenging, as it requires a large number of accurate tracer positions and radial velocities in the outer halo. The stellar halo of the Milky Way is probably the only target where this could become feasible in the future.

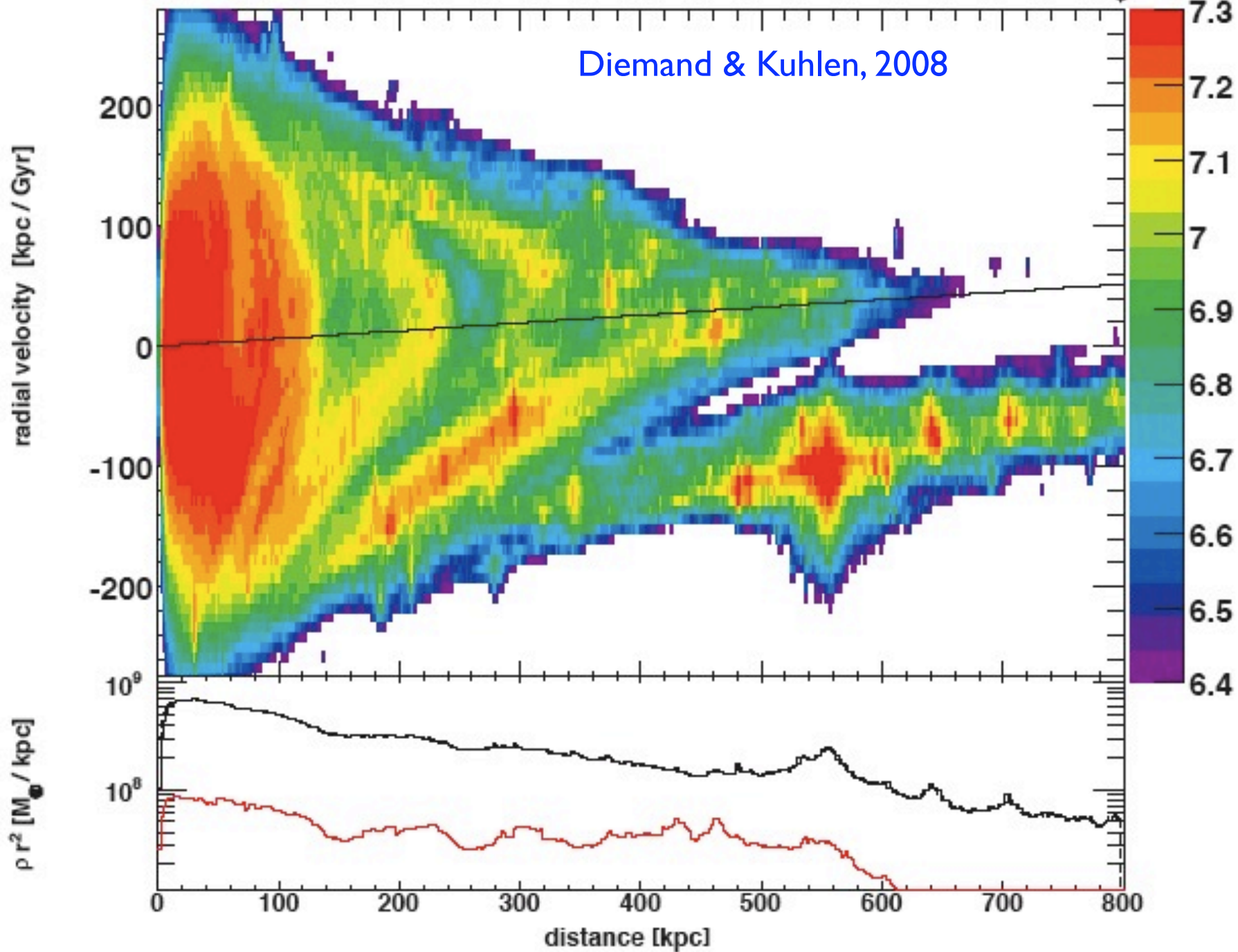
redshift 11.89

 $M_{\odot} \text{ kpc}^{-2} \text{ Gyr}$ 

redshift 0.00

$M_{\odot} \text{ kpc}^{-2} \text{ Gyr}$

Diemand & Kuhlen, 2008



## References

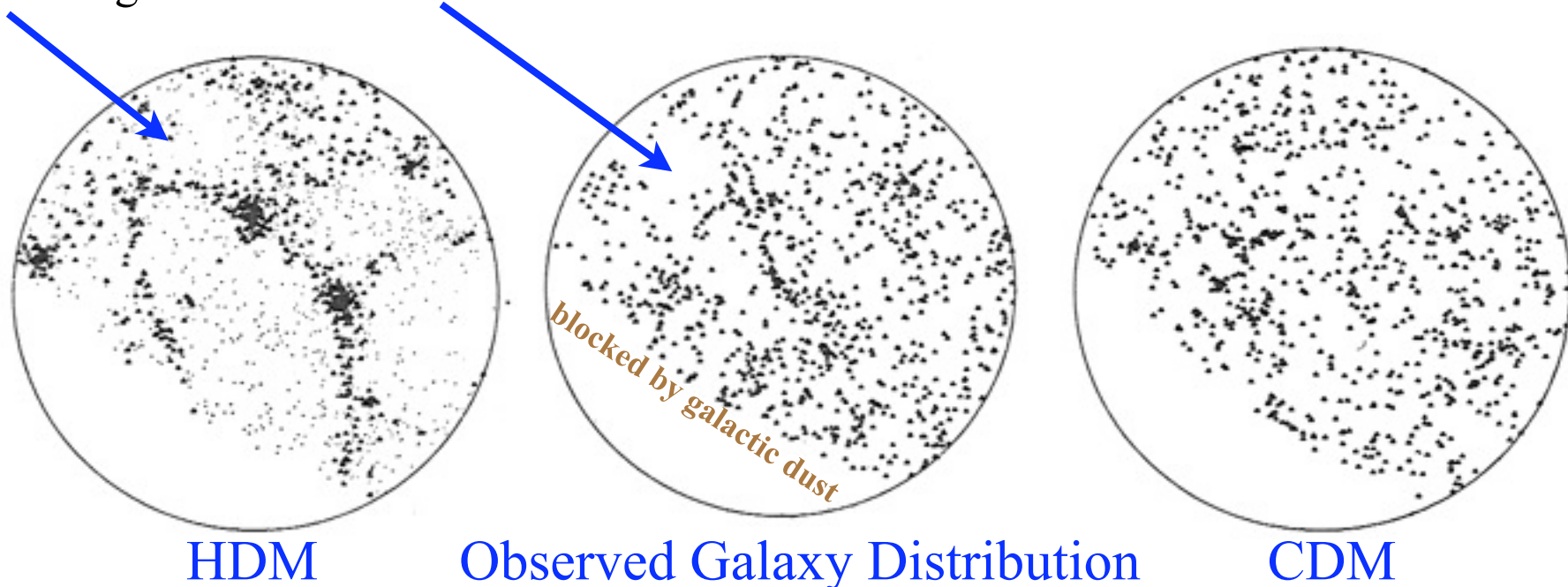
- [1] M. S. Turner, Phys. Rep. 197, 67 (1990). See also G. Raffelt, Lecture Notes in Physics, 741, 51 (2008) (arXiv:hep-ph/0611350).
- [2] D. Grin, G. Covone, J.-P. Kneib, M. Kamionkowski, A. Blain, and E. Jullo, Phys. Rev. D75, 105018 (2007).
- [3] P. Sikivie, Lecture Notes in Physics, 741, 19 (2008) (arXiv:astro-ph/0610440v2).
- [4] R. A. Battye and E. P. S. Shellard, Nucl. Phys. B423, 260 (1994); Phys. Rev. Lett. 73, 2954 (1994); (E) ibid. 76 (1996) 2203; arXiv:astro-ph/9909231. E. P. S. Shellard and R. A. Battye Nucl. Phys. B Proc. Supp. 72, 87 (1999).
- [5] P. Sikivie and Q. Yang, arXiv:0901.1106v2 (2009).
- [6] L. Carpenter, M. Dine, and G. Festuccia, arXiv:0906.1273v3 (2009).
- [7] A. Melissinos, Phys. Rev. Lett. 102, 202001 (2009) (arXiv:0807.1092).
- [8] S. J. Asztalos, L. J. Rosenberg, K. van Bibber, P. Sikivie, and K. Zioutas, Ann. Rev. Nucl. Part. Sci. 56, 293 (2006).
- [9] P. Sikivie, I. I. Tkachev, Y. Wang, Phys. Rev. Lett. 75, 2911 (1995); P. Sikivie, Phys. Lett. B432, 139 (1998); A. Natarajan and P. Sikivie, Phys. Rev. D72, 083513 (2005), Phys. Rev. D73, 023510 (2006); L. D. Duffy and P. Sikivie, Phys. Rev. D78, 063508 (2008).
- [10] J. Diemand and M. Kuhlen, ApJ Lett 680, L25 (2008). M. Zemp et al., MNRAS 394, 641 (2009). M. Vogelsberger, S. D. M. White, R. Mohayaee, and V. Springel, arXiv:0906.4341 (2009) and references therein.

# Some Dark Matter Candidates

axion	}	Weakly Interacting Massive Particles	}	COLD				
SUSY LSP neutralino								
technibaryon								
pseudo Higgs								
⋮								
shadow matter								
topological relics								
non-top. solitons								
Primordial BH					}	Massive Astrophysical Compact Halo Objects	}	DARK MATTER
jupiters								
brown dwarfs								
white dwarfs								
neutron stars								
stellar BH								
massive BH								
gravitino	}	WARM DM	}					
right-handed $\nu$								
decaying dark matter	}	VOLATILE DM	}					
⋮								
neutrinos $\nu_e \nu_\mu \nu_\tau (\nu_s?)$	}	HOT DARK MATTER	}					
majorons?								

# Whatever Happened to Hot Dark Matter?

In ~1980, when purely baryonic adiabatic fluctuations were ruled out by the improving upper limits on CMB anisotropies, theorists led by Zel'dovich turned to what we now call the HDM scenario, with light neutrinos making up most of the dark matter. However, in this scheme the fluctuations on small scales are damped by relativistic motion (“free streaming”) of the neutrinos until  $T$  becomes less than  $m_\nu$ , which occurs when the mass entering the horizon is about  $10^{15}$  solar masses, the supercluster mass scale. Thus superclusters would form first, and galaxies later by fragmentation. This predicted a galaxy distribution that would be much more inhomogeneous than observed.



Simon White, in *Inner Space/Outer Space* (1986)

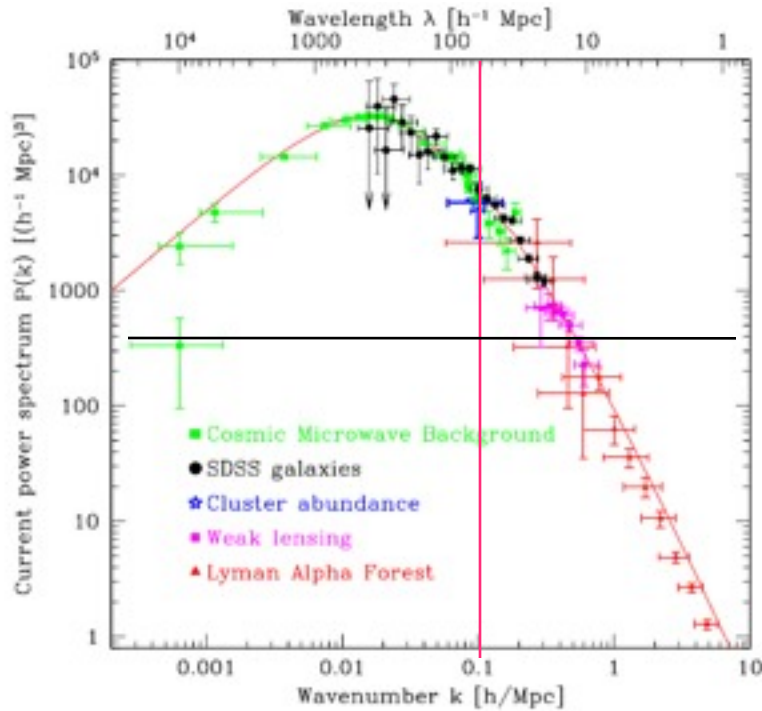
# Whatever Happened to Hot Dark Matter?

Since 1984, the most successful structure formation scenarios have been those in which most of the matter is CDM. With the COBE CMB data in 1992, two CDM variants appeared to be viable:  $\Lambda$ CDM with  $\Omega_m \approx 0.3$ , and  $\Omega_m = \text{Cold} + \text{Hot DM} = 1$  with  $\Omega_\nu \approx 0.2$  (Holtzman & Primack 1992, Wright et al. (COBE) 1992). Both cosmologies predicted a distribution of nearby galaxies in excellent agreement with observations.

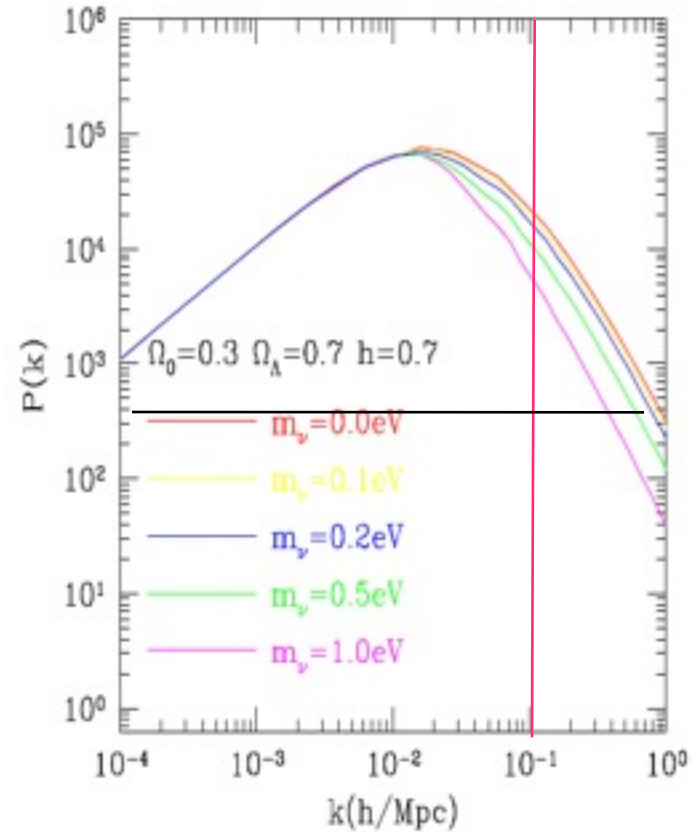
However, a potential problem with CHDM was that, like all  $\Omega_m = 1$  theories, it predicted rather late structure formation. By 1998, the evidence of early galaxy and cluster formation, the SN1a data showing that the expansion rate of the universe has been increasing, and the increasing evidence that  $\Omega_m \approx 0.3$  had favored  $\Lambda$ CDM and doomed CHDM.

Now we also know from neutrino oscillations that neutrinos have mass. The upper limit is  $\sum m_\nu < 1.3$  eV from CMB alone and  $\sum m_\nu < 0.44$  eV at 95% CL from CMB + LRG +  $H_0$  (WMAP7: Komatsu et al. 2010, Table 2). There is a stronger but somewhat controversial constraint  $\sum m_\nu < 0.17$  eV including Ly $\alpha$  forest data (Seljak et al. 2006).

# Effect of Neutrino Mass on Predicted Power Spectrum $P(k)$



SDSS  $P(k)$  Tegmark+05



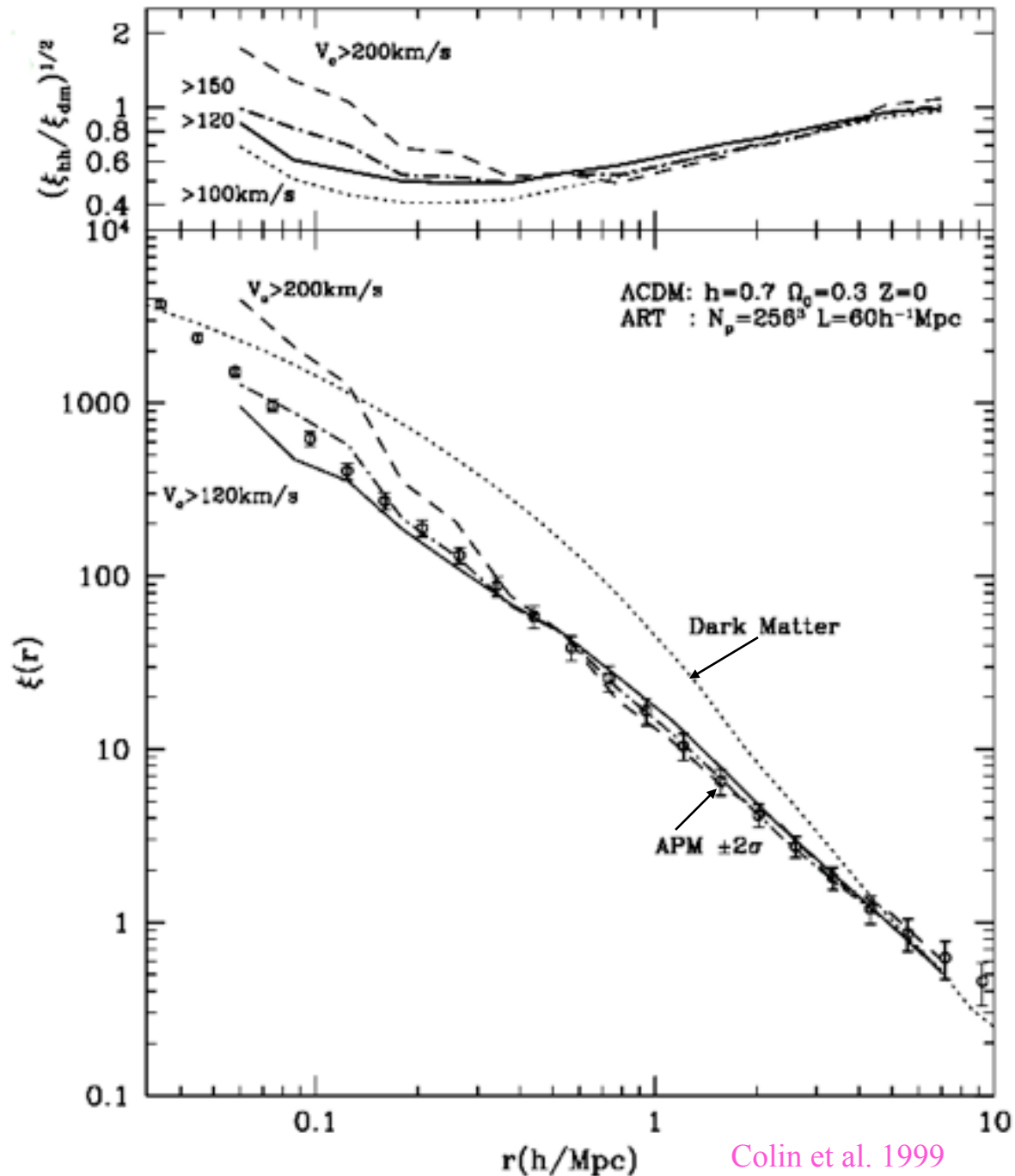
$P(k)$  for LCDM with degenerate neutrino masses totaling 1.0 eV or less.

**Masataka Fukugita, Massive Neutrinos in Cosmology**

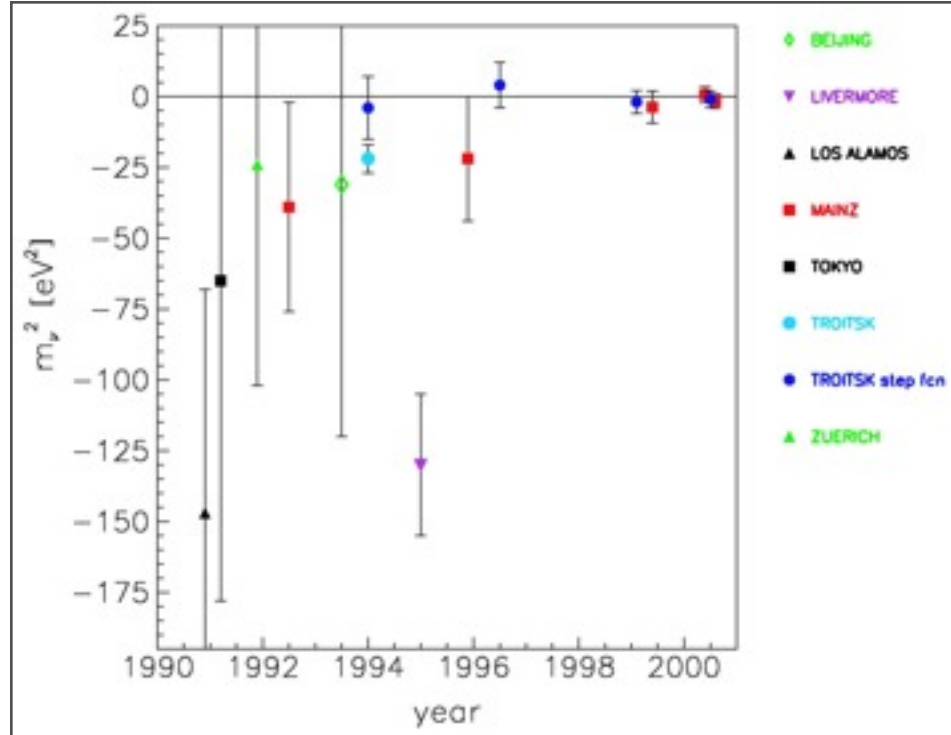
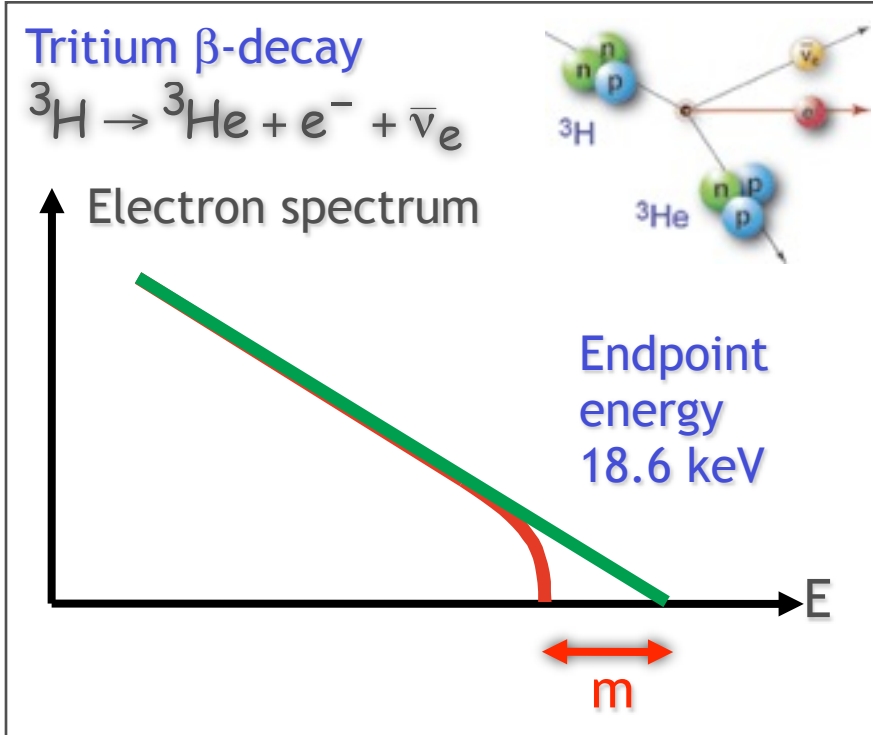
Plenary talk given at NuFact05, Frascati, 21-26 June 2005, [hep-ph/0511068](https://arxiv.org/abs/hep-ph/0511068)

# $\Lambda$ CDM Scale-Dependent Anti-Biasing

The dark matter correlation function  $\xi_{\text{mm}}$  for  $\Lambda$ CDM is  $\sim 3 \times \xi_{\text{gg}}$  at 1 Mpc. This disagreement between  $\xi_{\text{mm}}$  and  $\xi_{\text{gg}}$  was pointed out by Klypin, Primack, & Holtzman 1996. When simulations could resolve galaxy halos, it turned out that this needed “anti-biasing” arises naturally. This occurs because of destruction of halos in dense regions caused by merging and tidal disruption.



# $m(\nu_e)$ : Tritium Endpoint Spectrum



Currently best limits from Mainz and Troitsk experiments

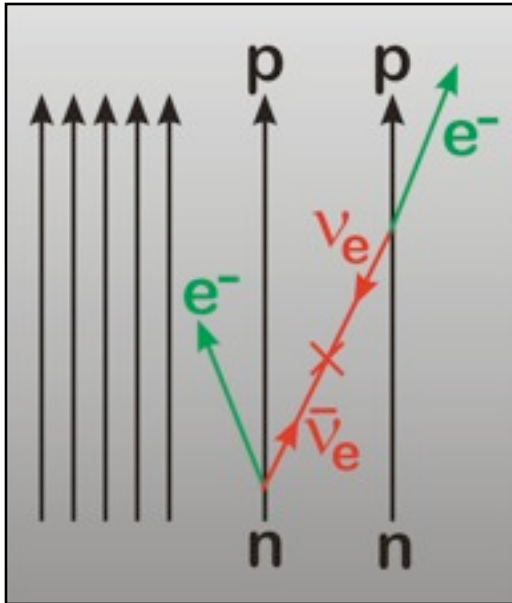
$$m < 2.2 \text{ eV (95\% CL)}$$

- Scaled-up spectrometer (KATRIN) should reach 0.2 eV
- Currently under construction
- Measurements to begin 2007

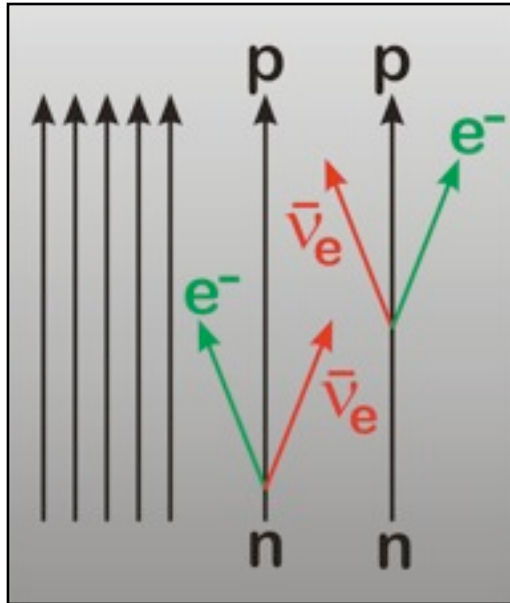
<http://ik1au1.fzk.de/~katrin>

# Neutrinoless $\beta\beta$ Decay

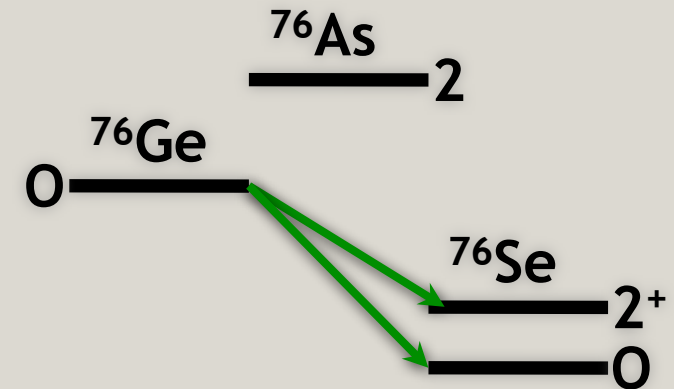
$0\nu$  mode, enabled by Majorana mass



Standard  $2\nu$  mode



Some nuclei decay only by the  $\beta\beta$  mode, e.g.



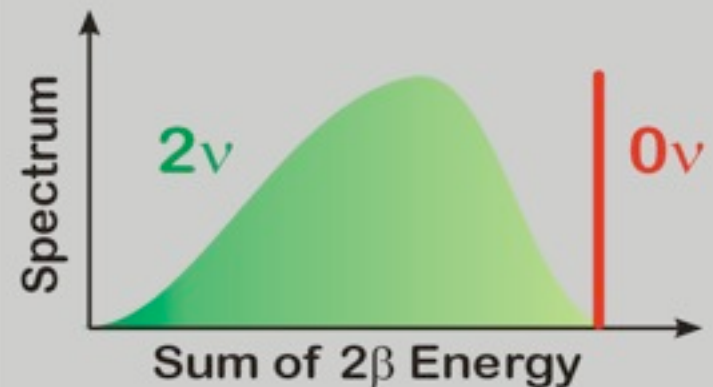
Half life  $\sim 10^{21}$  yr

Measured quantity

$$|m_{ee}| = \left| \sum_{i=1}^N \lambda_i |U_{ei}|^2 m_i \right|$$

Best limit from  $^{76}\text{Ge}$

$$|m_{ee}| < 0.35 \text{ eV}$$



## $\nu_e$

$$J = \frac{1}{2}$$

The following results are obtained using neutrinos associated with  $e^+$  or  $e^-$ . See the Note on “Electron, muon, and tau neutrino listings” in the Particle Listings.

Mass  $m < 3 \text{ eV}$  Interpretation of tritium beta decay experiments is complicated by anomalies near the endpoint, and the limits are not without ambiguity.

Mean life/mass,  $\tau/m_\nu > 7 \times 10^9 \text{ s/eV}$  [i] (solar)

Mean life/mass,  $\tau/m_\nu > 300 \text{ s/eV}$ , CL = 90% [i] (reactor)

Magnetic moment  $\mu < 1.0 \times 10^{-10} \mu_B$ , CL = 90%

## $\nu_\mu$

$$J = \frac{1}{2}$$

The following results are obtained using neutrinos associated with  $\mu^+$  or  $\mu^-$ . See the Note on “Electron, muon, and tau neutrino listings” in the Particle Listings.

Mass  $m < 0.19 \text{ MeV}$ , CL = 90%

Mean life/mass,  $\tau/m_\nu > 15.4 \text{ s/eV}$ , CL = 90%

Magnetic moment  $\mu < 6.8 \times 10^{-10} \mu_B$ , CL = 90%

## $\nu_\tau$

$$J = \frac{1}{2}$$

The following results are obtained using neutrinos associated with  $\tau^+$  or  $\tau^-$ . See the Note on “Electron, muon, and tau neutrino listings” in the Particle Listings.

Mass  $m < 18.2 \text{ MeV}$ , CL = 95%

Magnetic moment  $\mu < 3.9 \times 10^{-7} \mu_B$ , CL = 90%

Electric dipole moment  $d < 5.2 \times 10^{-17} \text{ e cm}$ , CL = 95%

## Number of Neutrino Types and Sum of Neutrino Masses

Number  $N = 2.994 \pm 0.012$  (Standard Model fits to LEP data)

Number  $N = 2.92 \pm 0.07$  (Direct measurement of invisible Z width)

## Neutrino Mixing

There is now compelling evidence that neutrinos have nonzero mass from the observation of neutrino flavor change, both from the study of atmospheric neutrino fluxes by SuperKamiokande, and from the study of solar neutrino cross sections by SNO (charged and neutral currents) and SuperKamiokande (elastic scattering). The flavor change observed in solar neutrinos has been confirmed by the KamLAND experiment using reactor antineutrinos.

### Solar Neutrinos

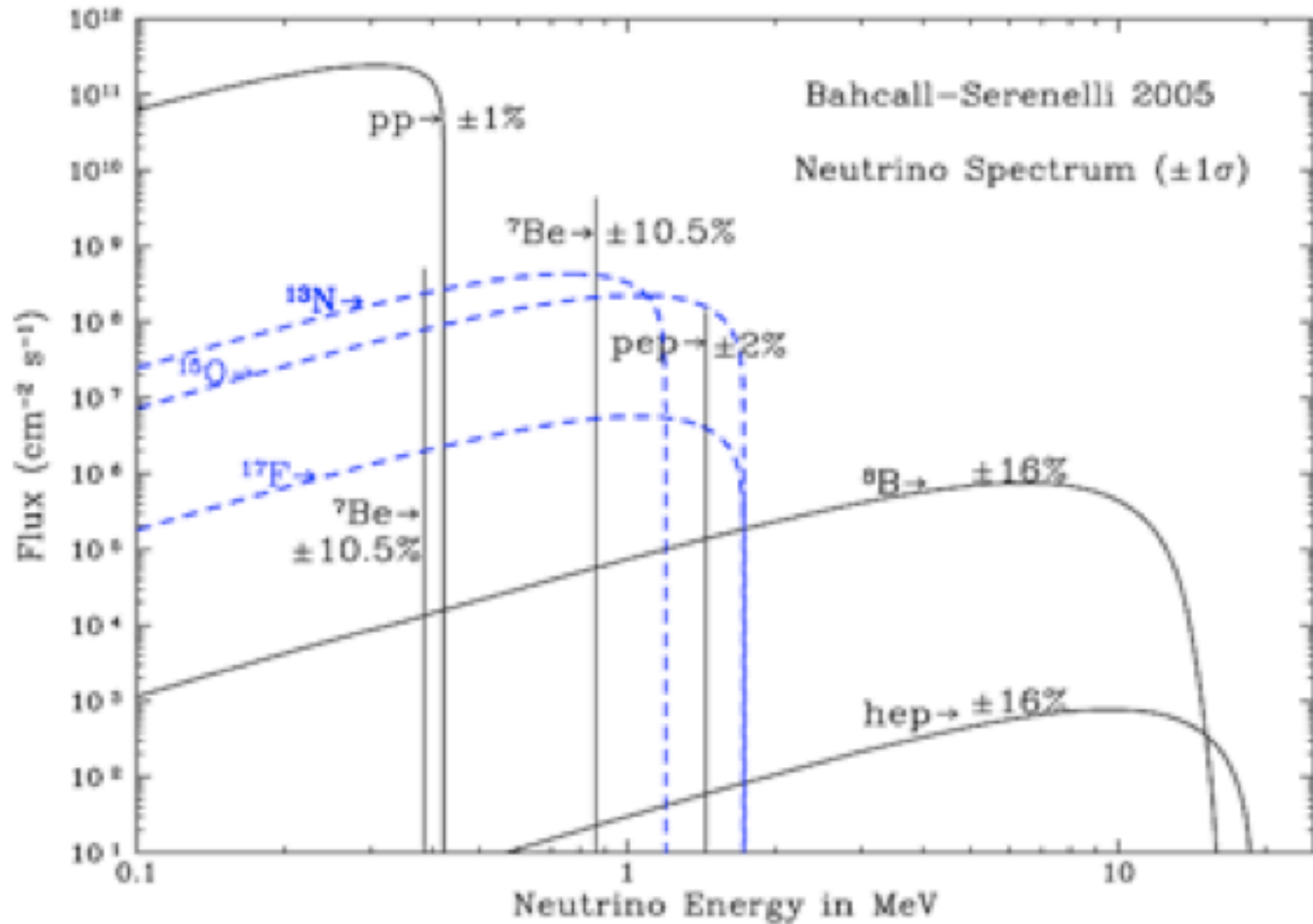
Detectors using gallium ( $E_\nu \gtrsim 0.2 \text{ MeV}$ ), chlorine ( $E_\nu \gtrsim 0.8 \text{ MeV}$ ), and Cherenkov effect in water ( $E_\nu \gtrsim 5 \text{ MeV}$ ) measure significantly lower neutrino rates than are predicted from solar models. From the determination by SNO of the  $^8\text{B}$  solar neutrino flux via elastic scattering, charged-current process interactions, and neutral-current interactions, one can determine the flux of non- $\nu_e$  active neutrinos to be  $\phi(\nu_{\mu\tau}) = (3.41_{-0.64}^{+0.66}) \times 10^6 \text{ cm}^{-2} \text{ s}^{-1}$ , providing a  $5.3\sigma$  evidence for neutrino flavor change. A global analysis of the solar neutrino data, including the KamLAND results that confirm the effect using reactor antineutrinos, favors large mixing angles and  $\Delta(m^2) \simeq (6-9) \times 10^{-5} \text{ eV}^2$ . See the Note “Solar Neutrinos” in the Listings and the review “Neutrino Mass, Mixing, and Flavor Change.”

### Atmospheric Neutrinos

Underground detectors observing neutrinos produced by cosmic rays in the atmosphere have measured a  $\nu_\mu/\nu_e$  ratio much less than expected, and also a deficiency of upward going  $\nu_\mu$  compared to downward. This can be explained by oscillations leading to the disappearance of  $\nu_\mu$  with  $\Delta m^2 \approx (1-3) \times 10^{-3} \text{ eV}^2$  and almost full mixing between  $\nu_\mu$  and  $\nu_\tau$ . The effect has been confirmed by the K2K experiment using accelerator neutrinos. See the review “Neutrino Mass, Mixing, and Flavor Change.”

Citation: S. Eidelman *et al.* (Particle Data Group), Phys. Lett. B **592**, 1 (2004) (URL: <http://pdg.lbl.gov>)

# Predicted Solar Neutrino Spectrum



THE ATMOSPHERIC-NEUTRINO DATA from the Super-Kamiokande underground neutrino detector in Japan provide strong evidence of muon to tau neutrino oscillations, and therefore that these neutrinos have nonzero mass (see the article by John Learned in the Winter 1999 *Beam Line*, Vol. 29, No. 3). This result is now being confirmed by results from the K2K experiment, in which a muon neutrino beam from the KEK accelerator is directed toward Super-Kamiokande and the number of muon neutrinos detected is about as expected from the atmospheric-neutrino data (see article by Jeffrey Wilkes and Koichiro Nishikawa, this issue).

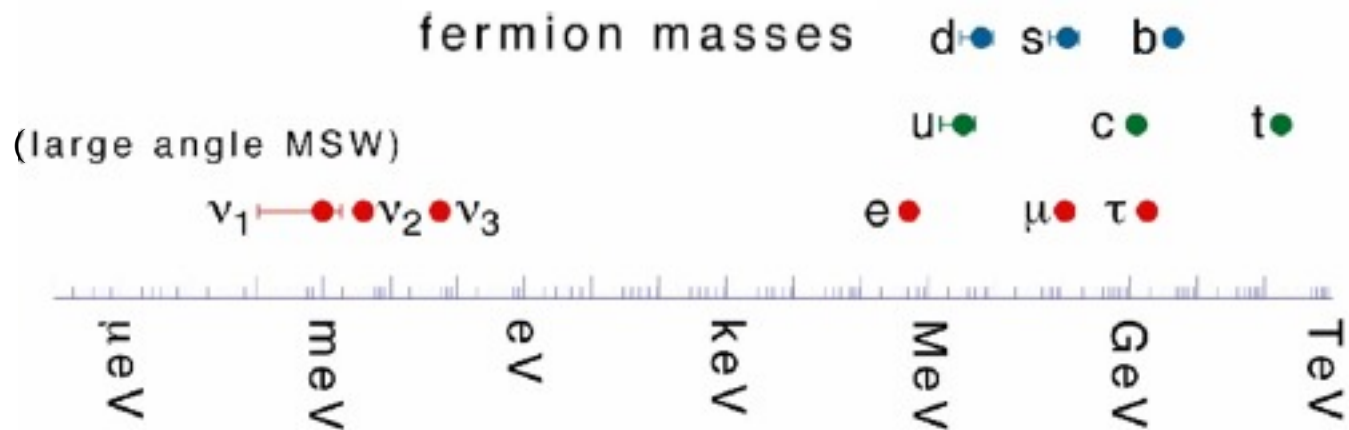
But oscillation experiments cannot measure neutrino masses directly, only the squared mass difference  $\Delta m_{ij}^2 = |m_i^2 - m_j^2|$  between the oscillating species. The Super-Kamiokande atmospheric neutrino data imply that  $1.7 \times 10^{-4} < \Delta m_{\tau\mu}^2 < 4 \times 10^{-3} \text{ eV}^2$  (90 percent confidence), with a central value  $\Delta m_{\tau\mu}^2 = 2.5 \times 10^{-3} \text{ eV}^2$ . If the neutrinos have a hierarchical mass pattern  $m_{\nu_e} \ll m_{\nu_\mu} \ll m_{\nu_\tau}$  like the quarks and charged leptons, then this implies that  $\Delta m_{\tau\mu}^2 \cong m_{\nu_\tau}^2$  so  $m_{\nu_\tau} \sim 0.05 \text{ eV}$ .

These data then imply a lower limit on the HDM (or light neutrino) contribution to the cosmological matter density of  $\Omega_\nu > 0.001$ —almost as much as that of all the stars in the disks of galaxies. There is a connection

between neutrino mass and the corresponding contribution to the cosmological density, because the thermodynamics of the early Universe specifies the abundance of neutrinos to be about 112 per cubic centimeter for each of the three species (including both neutrinos and antineutrinos). It follows that the density  $\Omega_\nu$  contributed by neutrinos is  $\Omega_\nu = m(\nu)/(93 h^2 \text{ eV})$ , where  $m(\nu)$  is the sum of the masses of all three neutrinos. Since  $h^2 \sim 0.5$ ,  $m_{\nu_\tau} \sim 0.05 \text{ eV}$  corresponds to  $\Omega_\nu \sim 10^{-3}$ .

This is however a lower limit, since in the alternative case where the oscillating neutrino species have nearly equal masses, the values of the individual masses could be much larger. The only other laboratory approaches to measuring neutrino masses are attempts to detect neutrino-less double beta decay, which are sensitive to a possible Majorana component of the electron neutrino mass, and measurements of the endpoint of the tritium beta-decay spectrum. The latter gives an upper limit on the electron neutrino mass, currently taken to be 3 eV. Because of the small values of both squared-mass differences, this tritium limit becomes an upper limit on all three neutrino masses, corresponding to  $m(\nu) < 9 \text{ eV}$ . A bit surprisingly, cosmology already provides a stronger constraint on neutrino mass than laboratory measurements, based on the effects of neutrinos on large-scale structure formation.

Joel Primack, *Beam Line*, Fall 2001



## Neutrino Properties

See the note on "Neutrino properties listings" in the Particle Listings.

$\nu_e$

Mass  $m < 2$  eV (tritium decay)

Mean life/mass,  $\tau/m > 300$  s/eV, CL = 90% (reactor)

Mean life/mass,  $\tau/m > 7 \times 10^9$  s/eV (solar)

Mean life/mass,  $\tau/m > 15.4$  s/eV, CL = 90% (accelerator)

Magnetic moment  $\mu < 0.9 \times 10^{-10} \mu_B$ , CL = 90% (reactor)

## Number of Neutrino Types

Number  $N = 2.994 \pm 0.012$  (Standard Model fits to LEP data)

Number  $N = 2.93 \pm 0.05$  ( $S = 1.2$ ) (Direct measurement of invisible Z width)

## Neutrino Mixing

The following values are obtained through data analyses based on the 3-neutrino mixing scheme described in the review "Neutrino mass, mixing, and flavor change" by B. Kayser in this *Review*.

$$\sin^2(2\theta_{12}) = 0.86^{+0.03}_{-0.04}$$

$$\Delta m_{21}^2 = (8.0^{+0.4}_{-0.3}) \times 10^{-5} \text{ eV}^2$$

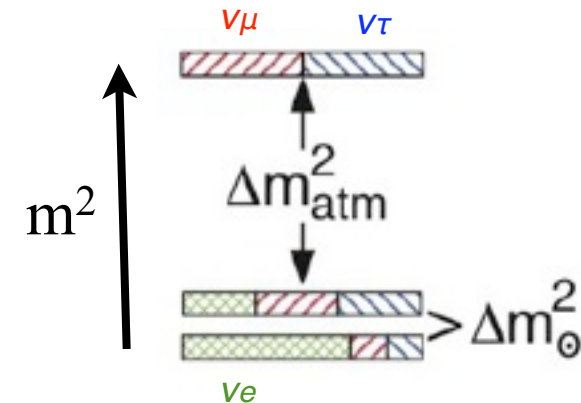
The ranges below for  $\sin^2(2\theta_{23})$  and  $\Delta m_{32}^2$  correspond to the projections onto the appropriate axes of the 90% CL contours in the  $\sin^2(2\theta_{23})$ - $\Delta m_{32}^2$  plane.

$$\sin^2(2\theta_{23}) > 0.92$$

$$\Delta m_{32}^2 = 1.9 \text{ to } 3.0 \times 10^{-3} \text{ eV}^2 [i]$$

$$\sin^2(2\theta_{13}) < 0.19, \text{ CL} = 90\%$$

Citation: W.-M. Yao *et al.*  
(Particle Data Group), J.  
Phys. G **33**, 1 (2006) (URL:  
<http://pdg.lbl.gov>)

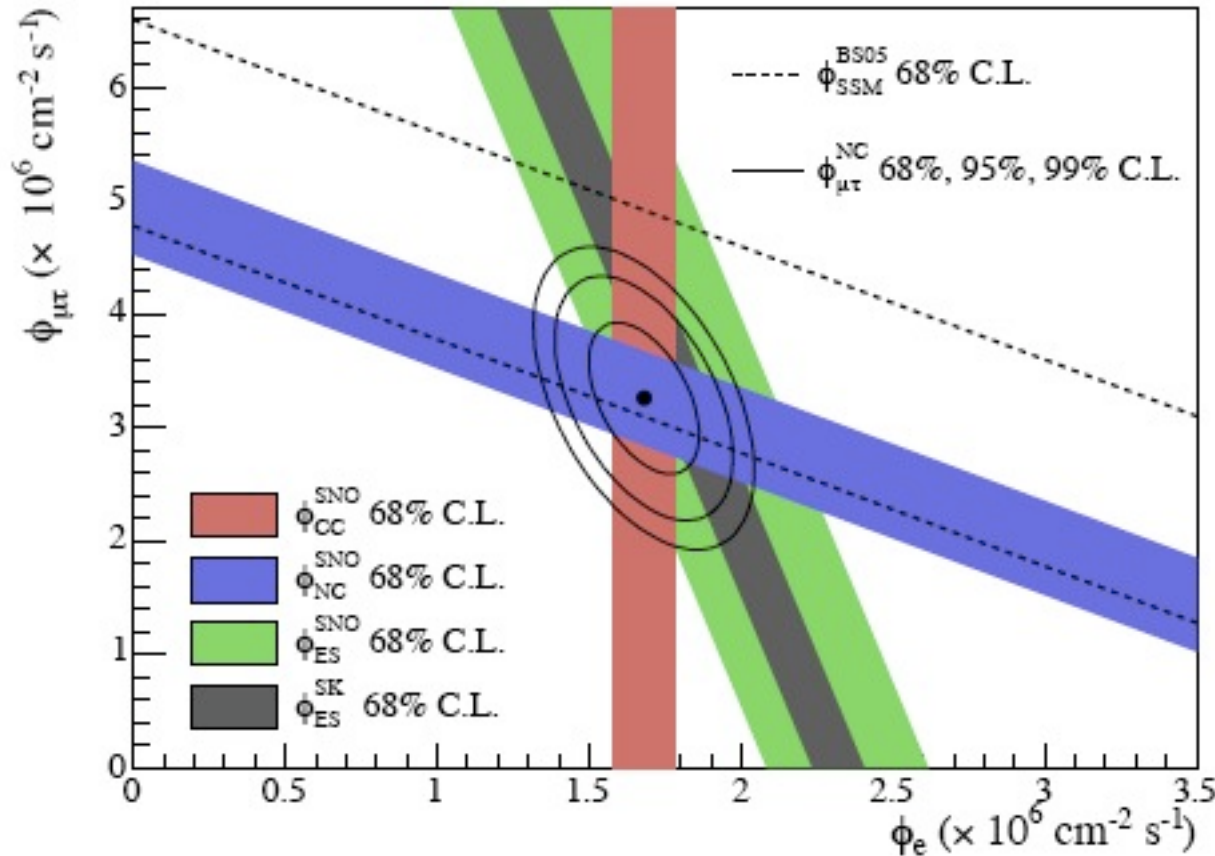


A three-neutrino squared-mass spectrum that accounts for the observed flavor changes of solar, reactor, atmospheric, and long-baseline accelerator neutrinos. The  $\nu_e$  fraction of each mass eigenstate is crosshatched, the  $\nu_\mu$  fraction is indicated by right-leaning hatching, and the  $\nu_\tau$  fraction by left-leaning hatching. From B. Kaiser, <http://pdg.lbl.gov/2007/reviews/>

[numixrpp.pdf](http://pdg.lbl.gov/2007/reviews/numixrpp.pdf)

# Sudbury Neutrino Observatory Confirms Solar Neutrinos Oscillate

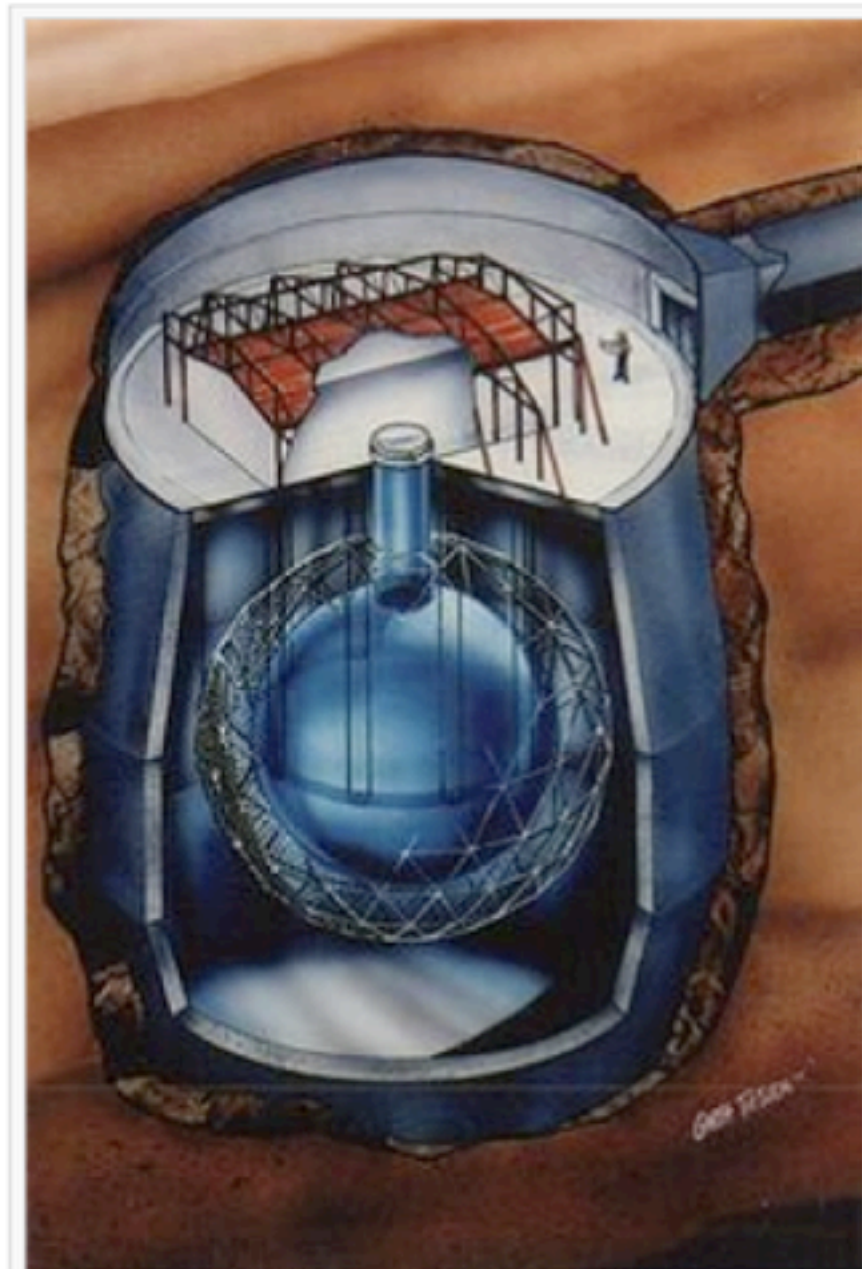
$n \rightarrow p e^- \bar{\nu}_e$  must happen twice per  ${}^4\text{He}$ , and then  $\sim 1/3$  of the electron antineutrinos oscillate to mu or tau neutrinos



Fluxes of  ${}^8\text{B}$  solar neutrinos,  $\phi(\nu_e)$ , and  $\phi(\nu_\mu \text{ or } \nu_\tau)$ , deduced from the SNO's charged current (CC),  $\nu_e$  elastic scattering (ES), and neutral-current (NC) results for the salt phase measurement. The Super-Kamiokande ES flux and the BS05(OP) standard solar model prediction are also shown. The bands represent the  $1\sigma$  error. The contours show the 68%, 95%, and 99% joint probability for  $\phi(\nu_e)$  and  $\phi(\nu_\mu \text{ or } \nu_\tau)$ .

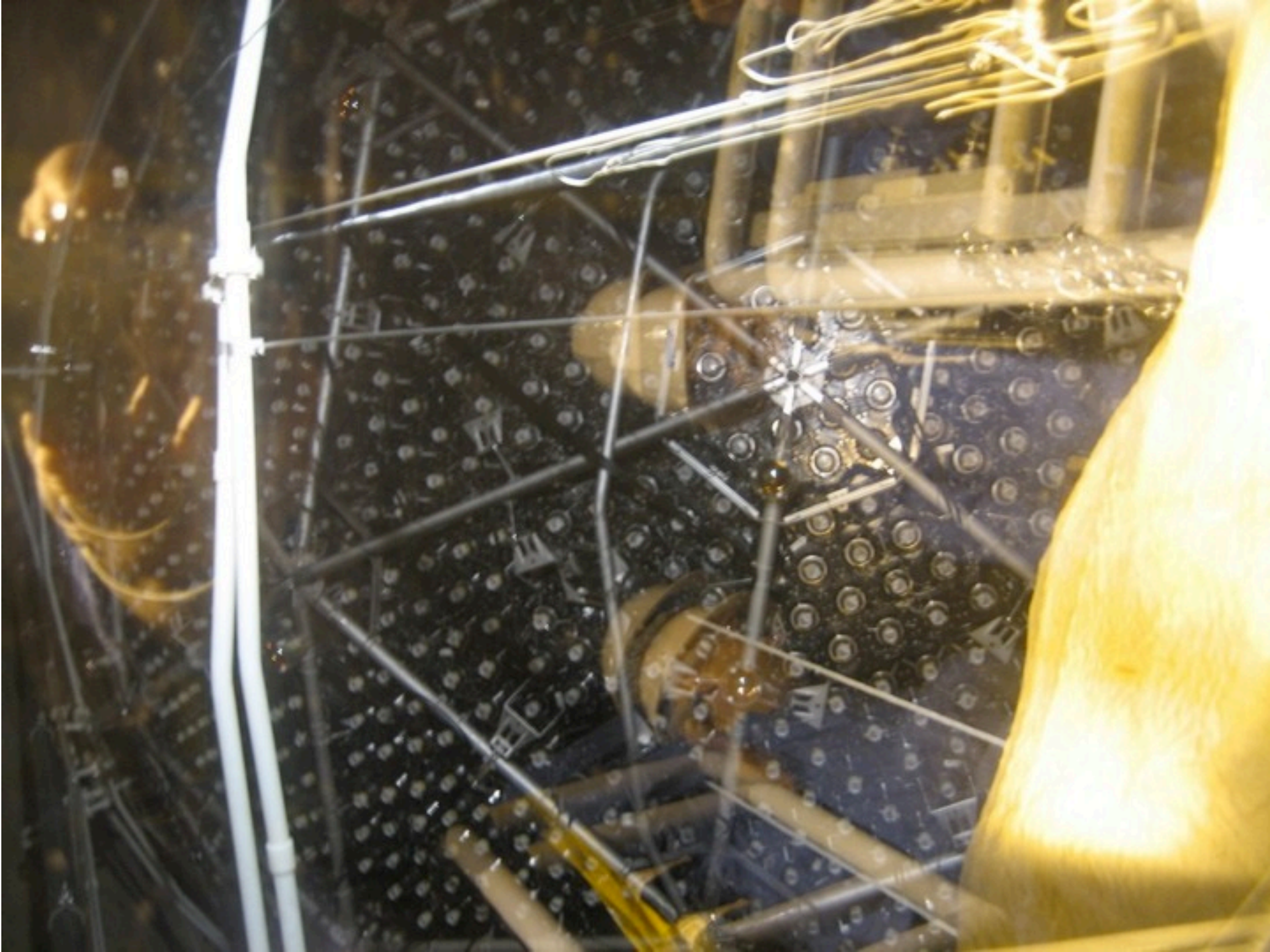
[From PDG 2005 review by K. Nakamura and 2009 rev.]

The **Sudbury Neutrino Observatory (SNO)** is a [neutrino observatory](#) located 6,800 feet (about 2 km) underground in [Vale Inco's Creighton Mine](#) in [Sudbury, Ontario, Canada](#). The detector was designed to detect [solar neutrinos](#) through their interactions with a large tank of [heavy water](#). The detector turned on in May 1999, and was turned off on 28 November 2006. While new data is no longer being taken the SNO collaboration will continue to analyze the data taken during that period for the next several years. The underground laboratory has been enlarged and continues to operate other experiments at [SNOLAB](#). The SNO equipment itself is currently being refurbished for use in the [SNO+](#) experiment.



Artist's concept of SNO's detector.







**SNO LAB**

MINING FOR KNOWLEDGE  
CREUSER POUR TROUVER... L'EXCELLENCE



UP  
BY ASSISTANT  
STATION  
DOWN

USE ONLY  
THE RADIO CAP LAMP THAT IS ASSIGNED TO YOU  
THESE RADIO CAP LAMPS ARE PERSONAL PROTECTIVE EQUIPMENT AND  
ARE MONITORED THROUGH THE SAFETY TRACK



REK  
M



**incênia**

DO  
NOT PUSH  
WITH  
FORKS

AUG 9

STORAGE  
SNO









### SEARCH FOR DARK MATTER WITH *Picasso*

**THE DARK MATTER PROBLEM**  
Astronomical observations show that only 5% of the matter in the universe is normal.  
95% of all matter consists of a new matter called dark matter (DM).  
DM was located during the Big Bang and is thought to account for most of the matter in the universe.

**THE PICASSO EXPERIMENT**  
The sensitive detector of the detector and millions of tiny 1000 electron photons of a supercooled liquid  $^3\text{He}$ .  
A liquid is supercooled when it is cooled well below its boiling point. Heat is taken in without boiling and a slight perturbation triggers an ionization-transformation-like response.  
The ionization rate (e.g.,  $10^4$  above in a bubble) is highly sensitive to the amount of energy that is recorded by photoelectric particles.

**HOW TO USE FUTURE PLANS**  
As a 10-ton detector with  $10^4$  active He atoms of  $^3\text{He}$ , PICASSO will be installed in an ultra-cold environment. Signals are recorded by a small number of photomultiplier tubes and read out by a computer system. Signals are recorded by a small number of photomultiplier tubes and read out by a computer system.

**WHY WE NEED TO FIND DARK MATTER**  
The dark matter problem is one of the most important unsolved problems in physics. The detection of dark matter would be a major step towards understanding the universe.

**THE PICASSO EXPERIMENT**  
The sensitive detector of the detector and millions of tiny 1000 electron photons of a supercooled liquid  $^3\text{He}$ .  
A liquid is supercooled when it is cooled well below its boiling point. Heat is taken in without boiling and a slight perturbation triggers an ionization-transformation-like response.  
The ionization rate (e.g.,  $10^4$  above in a bubble) is highly sensitive to the amount of energy that is recorded by photoelectric particles.

**WHY WE NEED TO FIND DARK MATTER**  
The dark matter problem is one of the most important unsolved problems in physics. The detection of dark matter would be a major step towards understanding the universe.

# SEARCH FOR DARK MATTER WITH

# Picasso

## THE DARK MATTER PROBLEM

Astronomical observations show that only 1% of the matter of the Universe is luminous.



25% of all matter should be of a new exotic kind: Cold Dark Matter (CDM)!



CDM was created during the Big Bang and is thought to surround most galaxies in huge clouds.

## THE PICASSO EXPERIMENT

The sensitive material of the detector are millions of tiny 100  $\mu\text{m}$  size droplets of a superheated liquid ( $\text{C}_4\text{F}_{10}$ ).

A liquid is superheated when it is heated well above its boiling point. Such a liquid is extremely unstable and a slight perturbation triggers an explosive transformation into vapour.

If a neutralino hits e.g. a F- atom in a droplet, a bubble forms and the acoustic signal will be recorded by piezo electric sensors



Set up of the first PICASSO prototype detectors at SNO. The detectors are surrounded by water cubes to shield the experiment from neutrons due to the natural radioactivity from the surrounding rock.



A 4.5l module with 80g of active mass of  $\text{C}_4\text{F}_{10}$ . Droplets are suspended in an elastic polymer. Signals are recorded by 9 piezo electric sensors. Events are localised by GPS-like triangulation.

Presently PICASSO is installing a new experiment with 32 detector modules and an active mass of 2 kg.

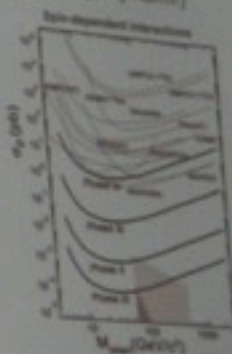


## NEUTRALINO DARK MATTER

The most favored candidate for CDM is the Neutralino. This hypothetical particle is neutral, 100x heavier than the proton and interacts very weakly with ordinary matter.

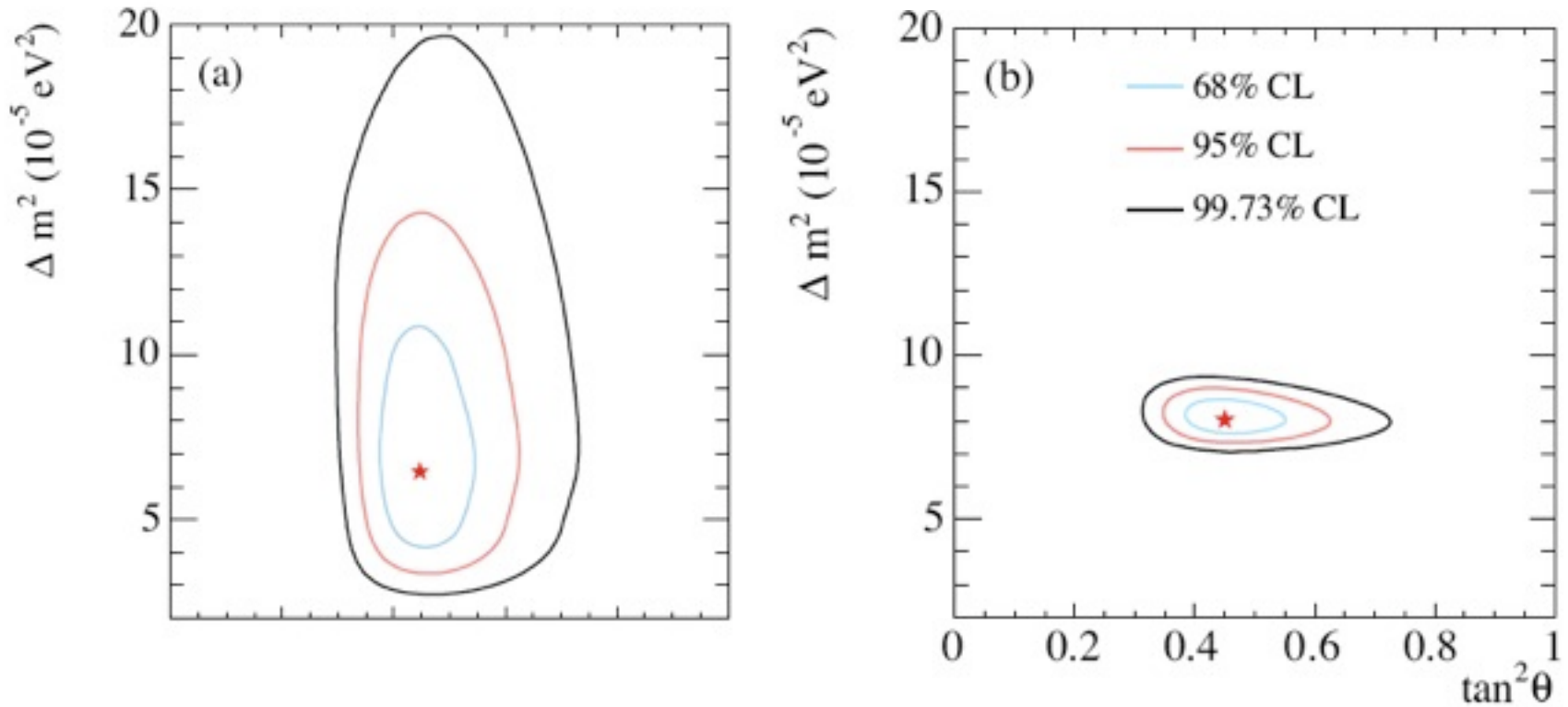
The earth moves with the sun around the center of the Milky Way within a huge cloud of neutralinos.

We guess that every minute about four million neutralinos traverse our body (without doing any harm!)



## RESULTS AND FUTURE PLANS

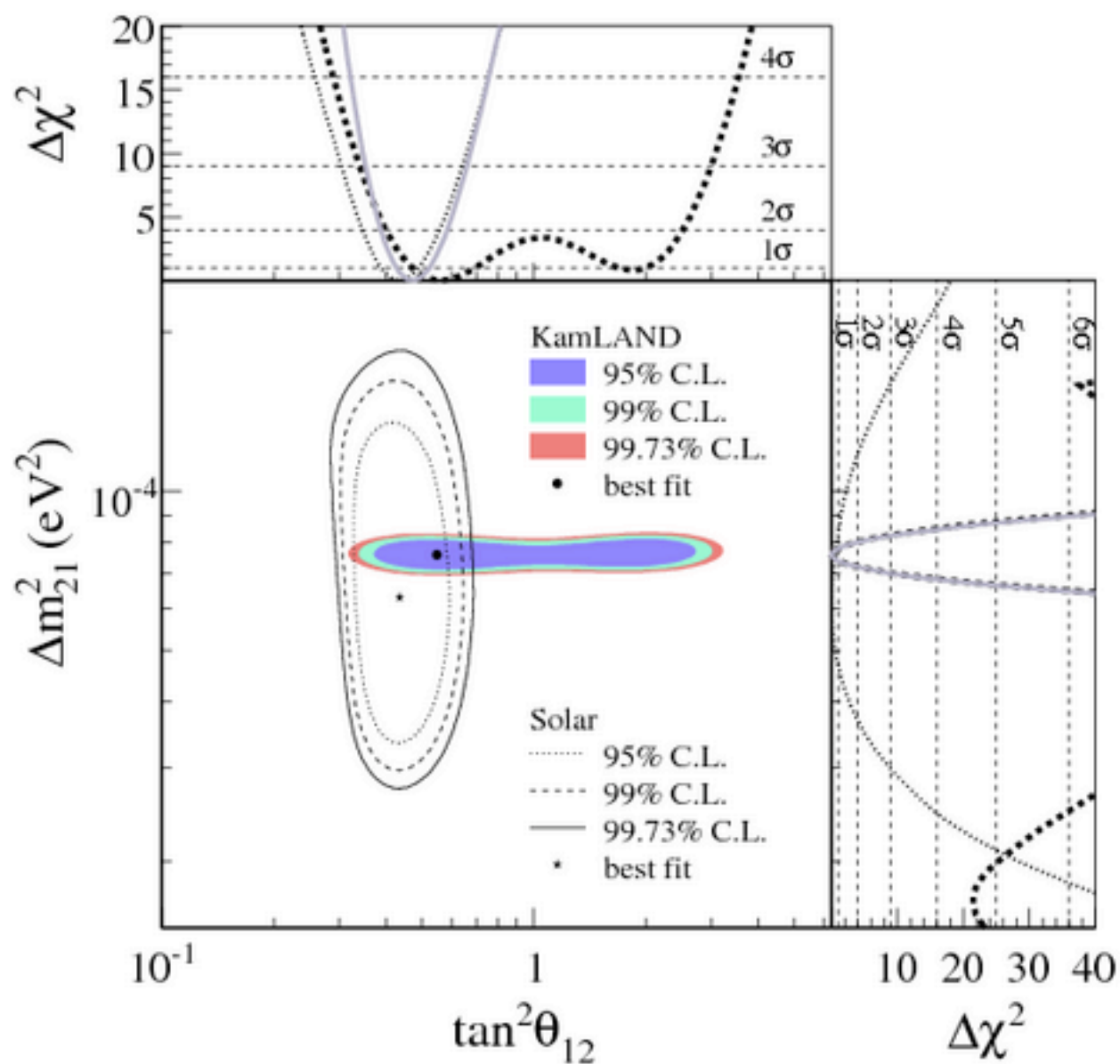
No CDM signal was found up to now! However limits for the interaction probability as a function of neutralino mass have been obtained. Future stages of PICASSO will be able to explore much weaker neutralino signals.



Update of the global neutrino oscillation contours given by the SNO Collaboration assuming that the  $^8\text{B}$  neutrino flux is free and the *hep* neutrino flux is fixed. (a) Solar global analysis. (b) Solar global + KamLAND. [From PDG 2005 review by K. Nakamura, and 2009 revision.]

$$\Delta m_{12}^2 = 8 \times 10^{-5} \text{ eV}^2 \Rightarrow m_2 \geq 9 \times 10^{-3} \text{ eV}$$

# Precision Measurement of Neutrino Oscillation Parameters with KamLAND



# KamLAND

KamLAND (*Kamioka Liquid-scintillator Anti-Neutrino Detector*) has demonstrated convincingly that neutrinos are massive and undergo flavour oscillations. This is a profound discovery !

The experiment has determined the associated oscillation parameter  $\Delta m^2_{21}$  to unprecedented precision, has helped constrain the neutrino mixing angle  $\theta_{12}$ , and has explored the potential application of neutrinos as a geophysical probe. The detector is currently undergoing a purification upgrade which will enable KamLAND to execute a low energy solar neutrino program in parallel with this already highly fruitful anti-neutrino program.

Many questions of fundamental significance remain open; but with a new understanding of neutrino propagation, neutrino science is now poised to provide illuminating answers to some of society's most probing questions concerning the Earth, the Sun and fantastic astro-physical events such as supernovae.

## The Reactor Neutrino Signal

The dominant sources of anti-neutrinos for the KamLAND experiment are commercial nuclear reactors in Japan. The average distance,  $L_0$ , from the reactors to the KamLAND detector is  $\sim 180$ km. KamLAND measures the survival probability by measuring the flux at the detector and comparing it to the known flux produced by the reactors. Anti-neutrinos are detected using the *delayed coincidence* method arising from inverse beta decay. Upon entering KamLAND, an electron anti-neutrino may capture on a free proton in the hydro-carbon based scintillator. The following reaction, known as inverse beta decay, then occurs:



The positron quickly ( $\sim 10$ 's ns) deposits its energy and then annihilates. The energy associated with this *prompt* event is directly related to the incoming neutrino energy. The remaining neutron thermalises and then later ( after  $\sim 200$ s  $\mu$  s) captures on proton yielding a deuteron and a  $\downarrow$  2.2MeV photon.

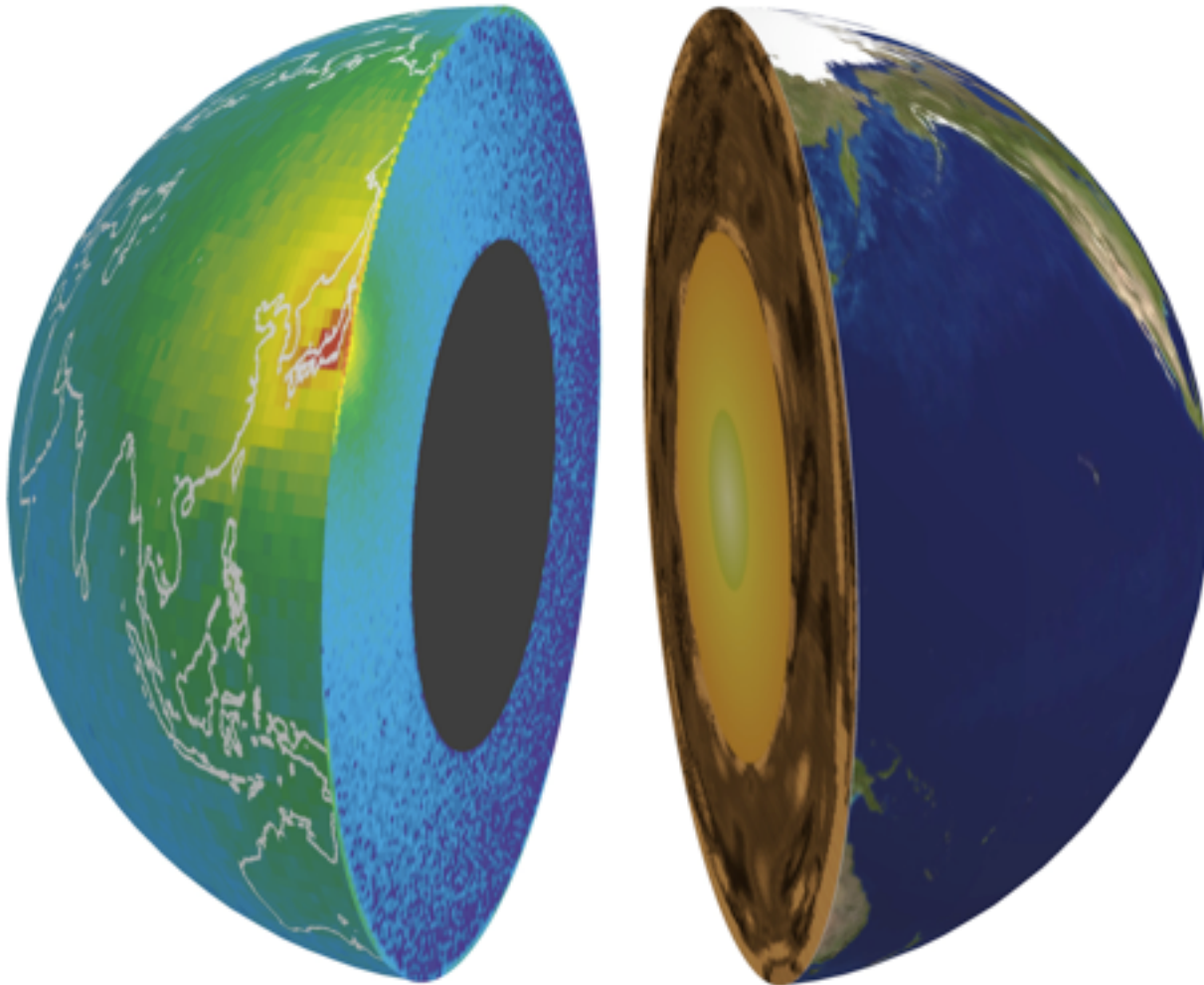


This neutron capture event is called the *delayed* event.

The delayed coincidence of the prompt and delayed event pair is an extremely robust signature of an anti-neutrino.

## Geo-Neutrinos

KamLAND has seen indications for geologically produced anti-neutrinos arising from uranium and thorium decays within the earth. Precision global measurements of the geo-neutrino flux can provide important and otherwise unattainable information about the composition and radiogenic heating of the earth's core. While this approach is still in its infancy, the KamLAND measurement was an important milestone in establishing its feasibility. There is considerable interest and excitement in the geological and physics communities about developing this technique to its full potential.



# Outline

Grand Unification of Forces

Phase Transitions in the Early Universe

Topological Defects: Strings, Monopoles\*

Cosmic Inflation (introduction)

\*Note: I edited much of the material in the following Topological Defects slides from the website [http://www.damtp.cam.ac.uk/user/gr/public/cs\\_top.html](http://www.damtp.cam.ac.uk/user/gr/public/cs_top.html)

# Grand Unification

The basic premise of grand unification is that the known symmetries of the elementary particles result from a larger (and so far unknown) symmetry group  $G$ . Whenever a phase transition occurs, part of this symmetry is lost, so the symmetry group changes. This can be represented mathematically as

$$G \rightarrow H \rightarrow \dots \rightarrow SU(3) \times SU(2) \times U(1) \rightarrow SU(3) \times U(1).$$

Here, each arrow represents a symmetry breaking phase transition where matter changes form and the groups -  $G$ ,  $H$ ,  $SU(3)$ , etc. - represent the different types of matter, specifically the symmetries that the matter exhibits and they are associated with the different fundamental forces of nature.

The liquid phase of water is rotationally symmetric, that is, it looks the same around each point regardless of the direction in which we look. We could represent this large three-dimensional symmetry by the group  $G$  (actually  $SO(3)$ ). The solid form of frozen water, however, is not uniform in all directions; the ice crystal has preferential lattice directions along which the water molecules align. The group describing these different discrete directions  $H$ , say, will be smaller than  $G$ . Through the process of freezing, therefore, the original symmetry  $G$  is broken down to  $H$ .

# Grand Unified Theory

**GUT** refers to a theory in physics that unifies the strong interaction and electroweak interaction. Several such theories have been proposed, but none is currently universally accepted. The (future) theory that will also include gravity is termed theory of everything. Some common GUT models are:

- Georgi-Glashow (1974) model --  $SU(5)$
- $SO(10)$
- Flipped  $SU(5)$  --  $SU(5) \times U(1)$
- Pati-Salam model --  $SU(4) \times SU(2) \times SU(2)$
- $E_6$

GUT models generically predict the existence of topological defects such as monopoles, cosmic strings, domain walls, and others. None have been observed and their absence is known as the monopole problem in cosmology.

There is still no hard evidence nature is described by a GUT theory. In fact, since the Higgs particle hasn't been discovered yet, it's not even certain if the Standard Model is fully accurate.

# Topological Defects

These arise when some n-component scalar field  $\phi_i(\mathbf{x}) = 0$  because of topological trapping that occurs as a result of a phase transition in the early universe (as I will explain shortly).

If the  $\phi$  field is complex then  $n=2$ , and  $\phi_i(\mathbf{x}) = 0$  occurs along a linear locus of points, a **string**, in three dimensional space. This corresponds to a 2-dimensional world-sheet in the 3+1 dimensions of spacetime.

If the  $\phi$  field has three components, then  $\phi_i(\mathbf{x}) = 0$  occurs at a point in three dimensional space, a **monopole**. This corresponds to a 1-dimensional world-line in the 3+1 dimensions of spacetime.

If the  $\phi$  field has four components, then  $\phi_i(\mathbf{x}) = 0$  occurs at a point in space-time, an **instanton**. A related concept is **texture**.

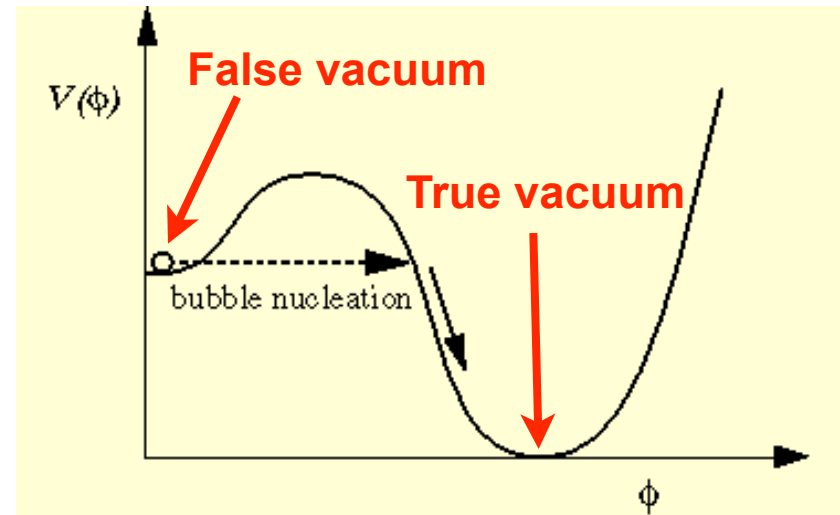
# Phase transitions

The cosmological significance of symmetry breaking is due to the fact that symmetries are restored at high temperature (just as it is for liquid water when ice melts). For extremely high temperatures in the early universe, we will even achieve a grand unified state G. Viewed from the moment of creation forward, the universe will pass through a succession of phase transitions at which the strong nuclear force will become differentiated and then the weak nuclear force and electromagnetism.

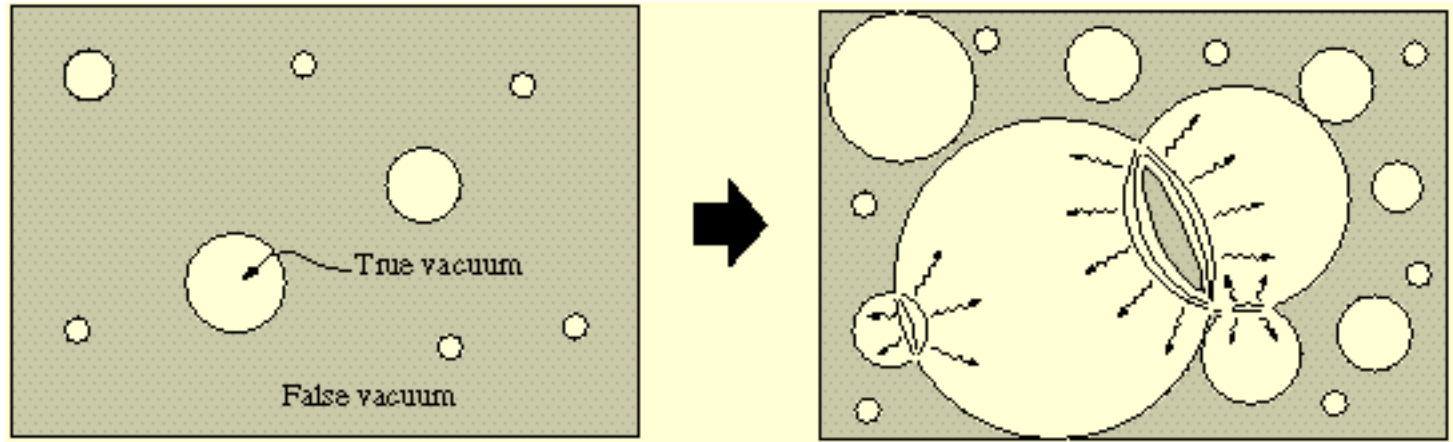
Phase transitions can have a wide variety of important implications including the formation of topological defects -cosmic strings, domain walls, monopoles and textures, or it may even trigger a period of exponential expansion (inflation).

Phase transitions can be either dramatic - first order - or smooth - second order.

During a first-order phase transition, the matter fields get trapped in a 'false vacuum' state from which they can only escape by nucleating bubbles of the new phase, that is, the 'true vacuum' state.



First-order phase transitions (illustrated below) occur through the formation of bubbles of the new phase in the middle of the old phase; these bubbles then expand and collide until the old phase disappears completely and the phase transition is complete.



First-order phase transitions proceed by bubble nucleation. A bubble of the new phase (the true vacuum) forms and then expands until the old phase (the false vacuum) disappears. A useful analogue is boiling water in which bubbles of steam form and expand as they rise to the surface.

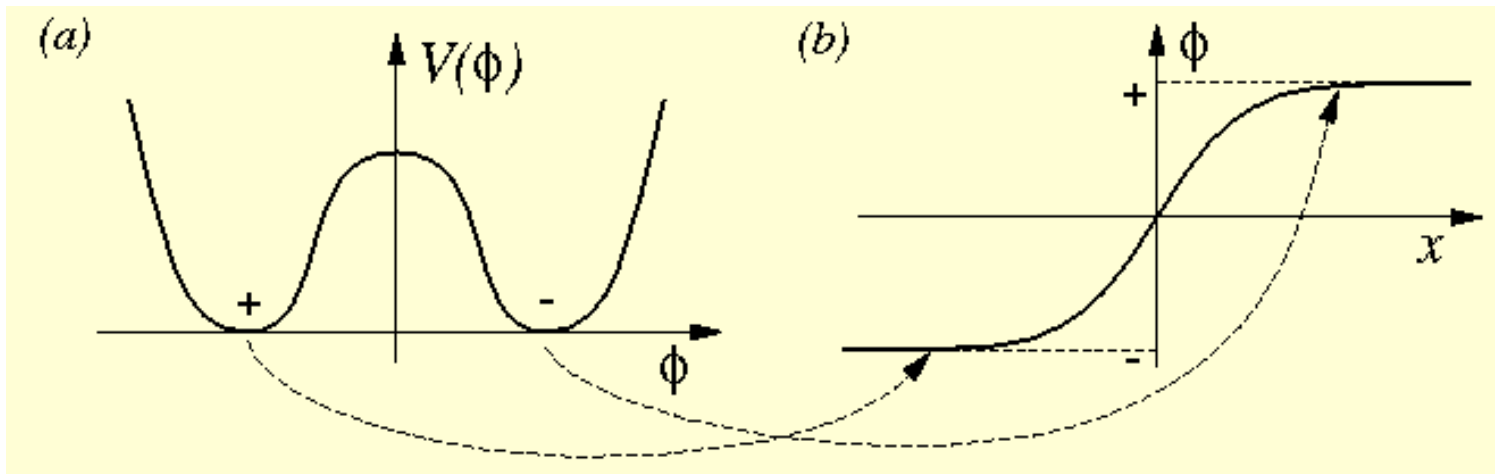
Second-order phase transitions, on the other hand, proceed smoothly. The old phase transforms itself into the new phase in a continuous manner. There is energy (specific heat of vaporization, for example) associated with a first order phase transition.

Either type of phase transition can produce stable configurations called “topological defects.”

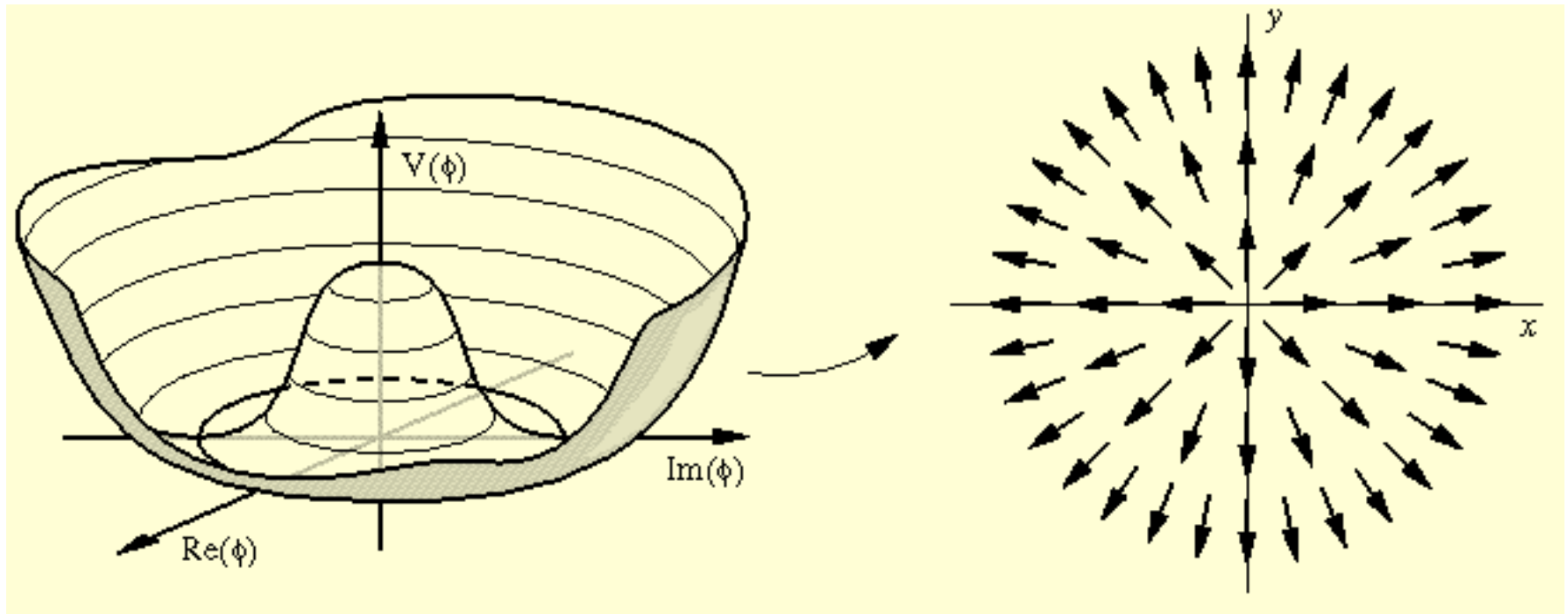
# Cosmic Strings & Other Topological Defects

Topological defects are stable configurations that are in the original, symmetric or old phase, but nevertheless for topological reasons they persist after a phase transition to the asymmetric or new phase is completed - because to unwind them would require a great deal of energy. There are a number of possible types of defects, such as domain walls, cosmic strings, monopoles, and textures. The type of defect is determined by the symmetry properties of the matter and the nature of the phase transition.

**Domain walls:** These are two-dimensional objects that form when a discrete symmetry is broken at a phase transition. A network of domain walls effectively partitions the universe into various 'cells'. Domain walls have some rather peculiar properties. For example, the gravitational field of a domain wall is repulsive rather than attractive.

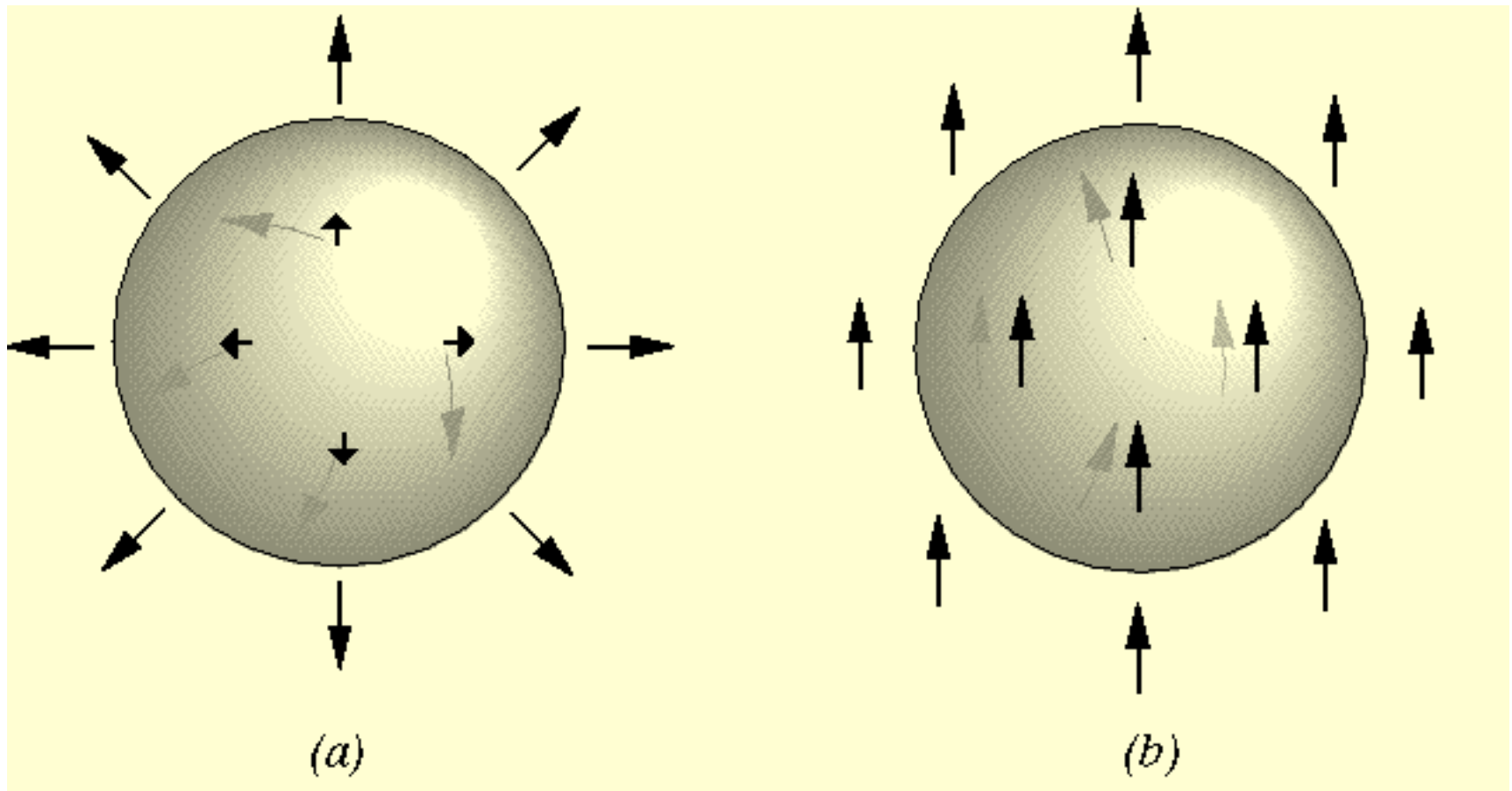


**Cosmic strings:** These are one-dimensional (that is, line-like) objects which form when an axial or cylindrical symmetry is broken. Strings can be associated with grand unified particle physics models, or they can form at the electroweak scale. They are very thin and may stretch across the visible universe. A typical GUT string has a thickness that is less than a trillion times smaller than the radius of a hydrogen atom, but a 10 km length of one such string would weigh as much as the earth itself!

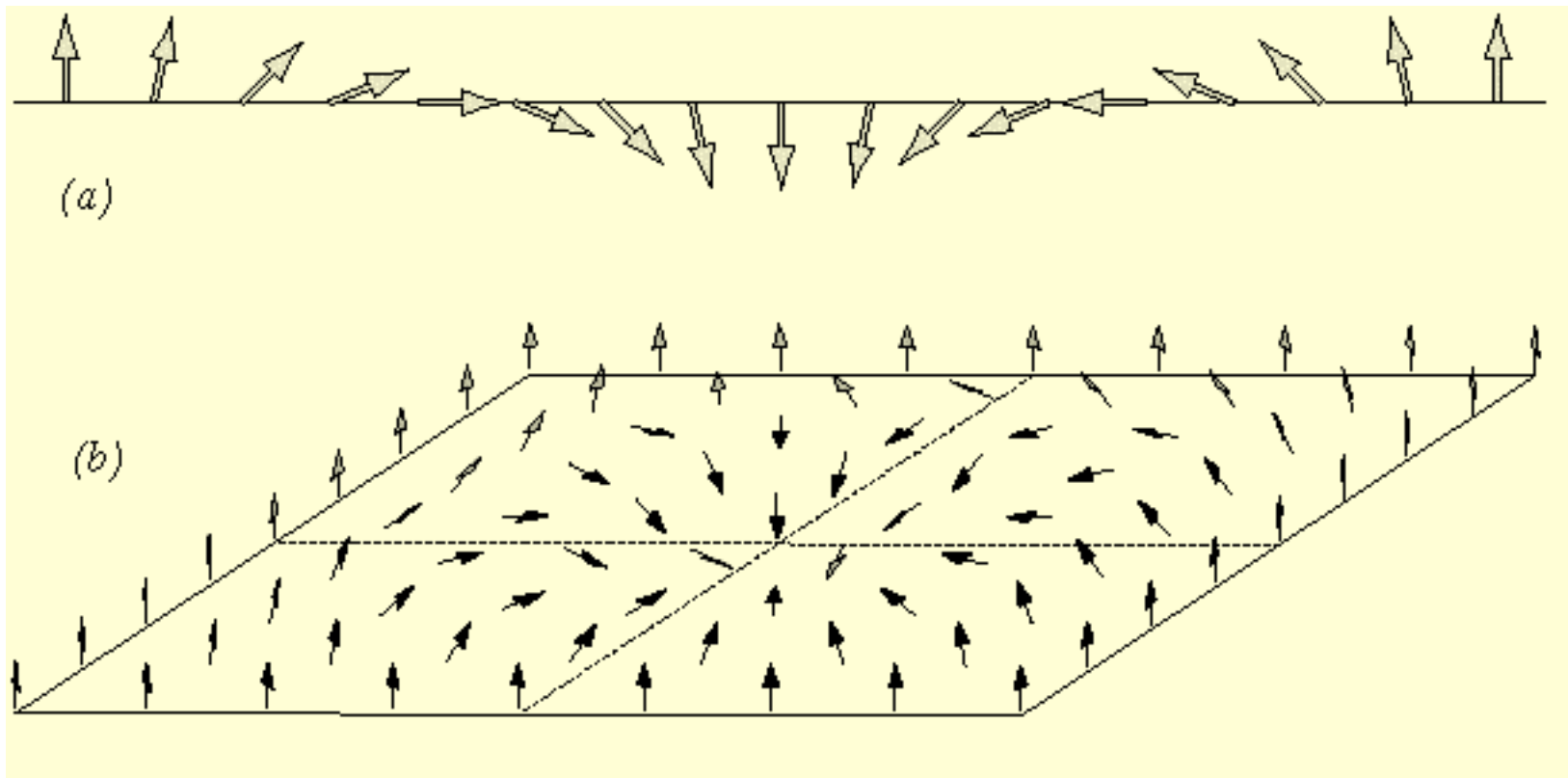


Cosmic strings are associated with models in which the set of minima are not simply-connected, that is, the vacuum manifold has 'holes' in it. The minimum energy states on the left form a circle and the string corresponds to a non-trivial winding around this.

**Monopoles:** These are zero-dimensional (point-like) objects which form when a spherical symmetry is broken. Monopoles are predicted to be supermassive and carry magnetic charge. The existence of monopoles is an inevitable prediction of grand unified theories (GUTs - more on this shortly); why the universe isn't filled with them is one of the puzzles of the standard cosmology.



**Textures:** These form when larger, more complicated symmetry groups are completely broken. Textures are delocalized topological defects which are unstable to collapse. A speculation that the largest “cold spot” in the WMAP CMB data was caused by cosmic textures was published by Cruz et al. (2007, Science 318, 1612).



Examples of delocalized texture configurations in one and two dimensions.

# CMB Lensing and the WMAP Cold Spot

Sudeep Das<sup>1,\*</sup> and David N. Spergel<sup>1,2,3,†</sup>

Cosmologists have suggested a number of intriguing hypotheses for the origin of the “WMAP cold spot”, the coldest extended region seen in the CMB sky, including a very large void and a collapsing texture. Either hypothesis predicts a distinctive CMB lensing signal. We show that the upcoming generation of high resolution CMB experiments such as ACT and SPT should be able to detect the signatures of either textures or large voids. If either signal is detected, it would have profound implications for cosmology.

Some theorists have speculated that the Cold Spot is a secondary effect, generated at some intermediate distance between us and the last scattering surface. One such model proposes that the Cold Spot may have been caused by the Rees-Sciama effect due to an underdense void of comoving radius  $\sim 200h^{-1}\text{Mpc}$  and fractional density contrast  $\delta \sim -0.3$  at redshift of  $z < 1$  [8, 9]. Interestingly, [10] reported a detection of an underdense region with similar characteristics in the distribution of extragalactic radio sources in the NRAO VLA Sky Survey in the direction of the Cold Spot, a claim which has recently been challenged [11]. An alternative view [12] proposes that the spot was caused by the interaction of the CMB photons with a cosmic texture, a type of topological defect that can give rise to hot and cold spots in the CMB [13]. Bayesian analysis by [14] claims that the texture hypothesis seems to be favored over the void explanation, mainly because such large voids as required by the latter is highly unlikely to form in a CDM structure formation scenario.

[8] K. T. Inoue and J. Silk, ApJ 648, 23 (2006), arXiv:astro-ph/0602478.

[9] K. T. Inoue and J. Silk, ApJ 664, 650 (2007), arXiv:astro-ph/0612347.

[10] L. Rudnick, S. Brown, and L. R. Williams, ApJ 671, 40 (2007).

[11] K. M. Smith and D. Huterer, ArXiv:0805.2751.

[12] M. Cruz, N. Turok, P. Vielva, E. Martínez-González, and M. Hobson, Science 318, 1612 (2007).

[13] N. Turok and D. Spergel, Physical Review Letters 64, 2736 (1990).

[14] M. Cruz, E. Martínez-González, P. Vielva, J. M. Diego, M. Hobson, and N. Turok, ArXiv:0804.2904.

# A Cosmic Microwave Background Feature Consistent with a Cosmic Texture

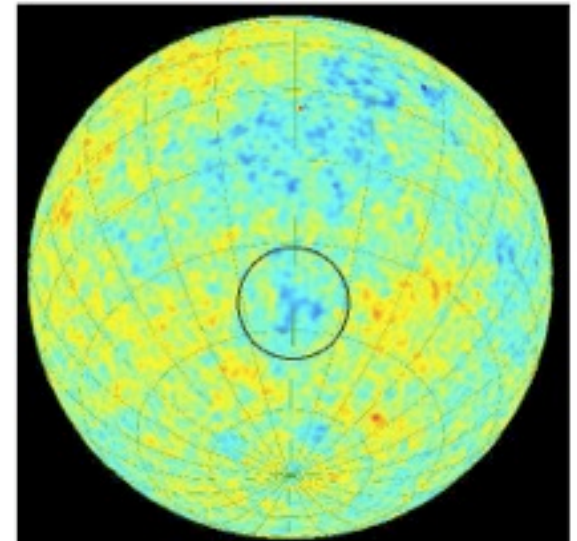
M. Cruz,<sup>1,2\*</sup> N. Turok,<sup>3</sup> P. Vielva,<sup>1</sup> E. Martínez-González,<sup>1</sup> M. Hobson<sup>4</sup> SCIENCE VOL 318 7 DECEMBER 2007

The Cosmic Microwave Background provides our most ancient image of the universe and our best tool for studying its early evolution. Theories of high-energy physics predict the formation of various types of topological defects in the very early universe, including cosmic texture, which would generate hot and cold spots in the Cosmic Microwave Background. We show through a Bayesian statistical analysis that the most prominent 5°-radius cold spot observed in all-sky images, which is otherwise hard to explain, is compatible with having been caused by a texture. From this model, we constrain the fundamental symmetry-breaking energy scale to be  $\phi_0 \approx 8.7 \times 10^{15}$  gigaelectron volts. If confirmed, this detection of a cosmic defect will probe physics at energies exceeding any conceivable terrestrial experiment.

## The Axis of Evil revisited

Kate Land, Joao Magueijo, 2007 MNRAS, 378, 153

Abstract: In light of the three-year data release from WMAP we re-examine the evidence for the "Axis of Evil" (AOE) [anomalous alignment of CMB multipoles in the direction  $l \approx -100$ ,  $b = 60$ ]. We discover that previous statistics are not robust with respect to the data-sets available and different treatments of the galactic plane. We identify the cause of the instability and implement an alternative "model selection" approach. A comparison to Gaussian isotropic simulations find the features significant at the 94-98% level, depending on the particular AOE model. The Bayesian evidence finds lower significance, ranging from "substantial" to no evidence for the most general AOE model.



The zone of the CS has been placed at the center of the black circle.

# The CMB cold spot: texture, cluster or void?

M. Cruz,<sup>1\*</sup> E. Martínez-González,<sup>1</sup> P. Vielva,<sup>1</sup> J. M. Diego,<sup>1</sup> M. Hobson,<sup>2</sup> N. Turok<sup>3</sup>

The non-Gaussian cold spot found in the WMAP data has created controversy about its origin. Here we calculate the Bayesian posterior probability ratios for three different models that could explain the cold spot. A recent work claimed that the Spot could be caused by a cosmic texture, while other papers suggest that it could be due to the gravitational effect produced by an anomalously large void. Also the Sunyaev-Zeldovich effect caused by a cluster is taken into account as a possible origin. We perform a template fitting on a  $20^\circ$  radius patch centered at Galactic coordinates ( $b = -57^\circ, l = 209^\circ$ ) and calculate the posterior probability ratios for the void and Sunyaev-Zeldovich models, comparing the results to those obtained with texture. Taking realistic priors for the parameters, the texture interpretation is favored, while the void and Sunyaev-Zeldovich hypotheses are discarded. The temperature decrement produced by voids or clusters is negligible considering realistic values for the parameters.

# Seven-Year Wilkinson Microwave Anisotropy Probe (WMAP) Observations: Are There Cosmic Microwave Background Anomalies? C. Bennett et al. WMAP7 Jan 2010

[arXiv:1001.4758v1](https://arxiv.org/abs/1001.4758v1)

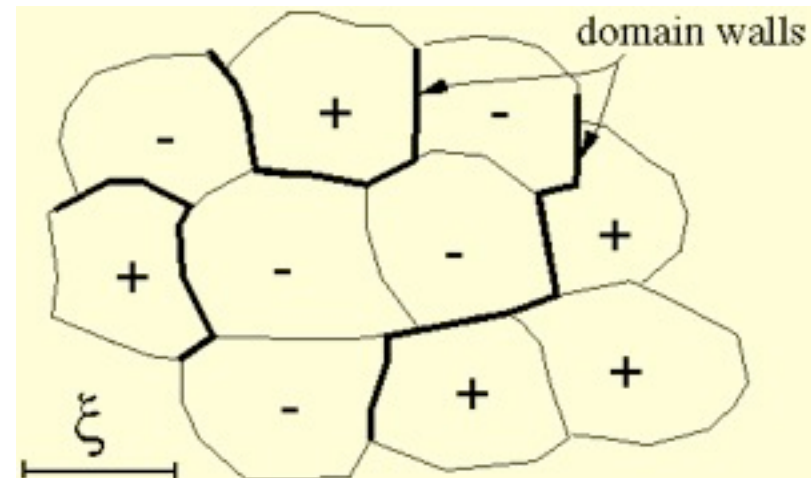
A simple six-parameter  $\Lambda$ CDM model provides a successful fit to WMAP data, both when the data are analyzed alone and in combination with other cosmological data. Even so, it is appropriate to search for any hints of deviations from the now standard model of cosmology, which includes inflation, dark energy, dark matter, baryons, and neutrinos. The cosmological community has subjected the WMAP data to extensive and varied analyses. While there is widespread agreement as to the overall success of the six-parameter  $\Lambda$ CDM model, various "anomalies" have been reported relative to that model. In this paper we examine potential anomalies and present analyses and assessments of their significance. In most cases we find that claimed anomalies depend on posterior selection of some aspect or subset of the data. Compared with sky simulations based on the best fit model, one can select for low probability features of the WMAP data. Low probability features are expected, but it is not usually straightforward to determine whether any particular low probability feature is the result of the a posteriori selection or of non-standard cosmology. We examine in detail the properties of the power spectrum with respect to the  $\Lambda$ CDM model. We examine several potential or previously claimed anomalies in the sky maps and power spectra, including cold spots, low quadrupole power, quadrupole-octupole alignment, hemispherical or dipole power asymmetry, and quadrupole power asymmetry. **We conclude that there is no compelling evidence for deviations from the  $\Lambda$ CDM model, which is generally an acceptable statistical fit to WMAP and other cosmological data.**

# Why do cosmic topological defects form?

If cosmic strings or other topological defects *can* form at a cosmological phase transition then they *will* form. This was first pointed out by Kibble and, in a cosmological context, the defect formation process is known as the **Kibble mechanism**.

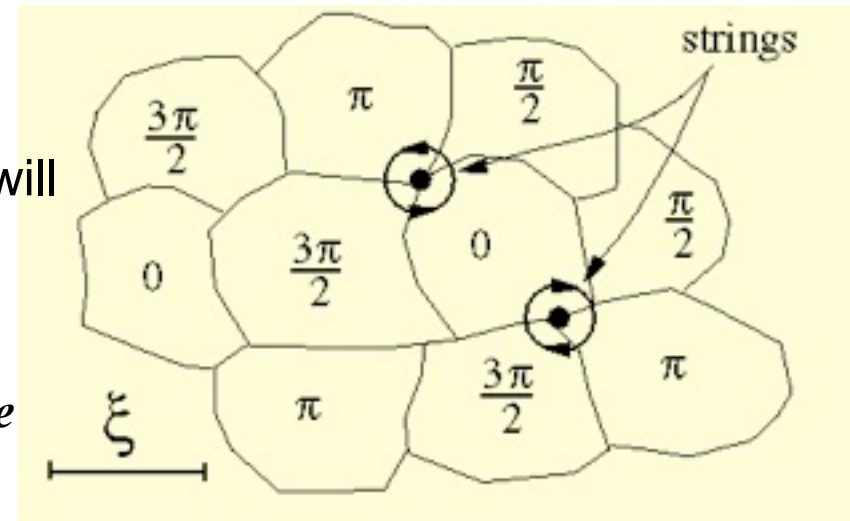
The simple fact is that causal effects in the early universe can only propagate (as at any time) at the speed of light  $c$ . This means that at a time  $t$ , regions of the universe separated by more than a distance  $d=ct$  can know nothing about each other. In a symmetry breaking phase transition, different regions of the universe will choose to fall into different minima in the set of possible states (this set is known to mathematicians as the vacuum manifold). Topological defects are precisely the “boundaries” between these regions with different choices of minima, and their formation is therefore an inevitable consequence of the fact that different regions cannot agree on their choices.

For example, in a theory with two minima, plus  $+$  and minus  $-$ , then neighboring regions separated by more than  $ct$  will tend to fall randomly into the different states (as shown below). Interpolating between these different minima will be a **domain wall**.



**Cosmic strings** will arise in slightly more complicated theories in which the minimum energy states possess 'holes'. The strings will simply correspond to non-trivial 'windings' around these holes (as illustrated at right).

*The Kibble mechanism for the formation of cosmic strings.*



Topological defects can provide a unique link to the physics of the very early universe. Furthermore, they can crucially affect the evolution of the universe, so their study is an unavoidable part of any serious attempt to understand the early universe. The **cosmological consequences** vary with the type of defect considered. Domain walls and monopoles are cosmologically catastrophic. Any cosmological model in which they form will evolve in a way that contradicts the basic observational facts that we know about the universe. Such models must therefore be ruled out! Cosmic inflation was invented to solve this problem.

Cosmic strings and textures are (possibly) much more benign. Among other things, they were until recently thought to be a possible source of the fluctuations that led to the formation of the large-scale structures we observe today, as well as the anisotropies in the Cosmic Microwave Background. However, the CMB anisotropies have turned out not to agree with the predictions of this theory.